Journal of Paleontology, 96(2), 2022, p. 462–484
Copyright © The Author(s), 2021. Published by Cambridge University Press on behalf of The Paleontological Society
0022-3360/22/1937-2337
doi: 10.1017/jpa.2021.93

JOURNAL OF PALEONTOLOGY
A PUBLICATION OF THE Paleontological SOCIETY

A new Late Devonian flora from Sonid Zuoqi, Inner Mongolia, northeastern China

Lingqi Bai,[1,2] Pu Huang,[3] Ning Yang,[3] Wenxin Ju,[4] Jianbo Liu,[1] James F. Basinger,[5] Honghe Xu,[3]* and Jinzhuang Xue[1]*

[1]School of Earth and Space Sciences, Peking University, Beijing 100871, China <bailingqi@pku.edu.cn> <jbliu@pku.edu.cn> <pkuxue@pku.edu.cn>
[2]Institute of Geology, Chinese Academy of Geological Sciences, Beijing 100037, China
[3]State Key Laboratory of Palaeobiology and Stratigraphy, Nanjing Institute of Geology and Palaeontology, and Center for Excellence in Life and Paleoenvironment, Chinese Academy of Sciences, Nanjing 210008, China <puhuang@nigpas.ac.cn> <ningyang@nigpas.ac.cn> <hhxu@nigpas.ac.cn>
[4]Inner Mongolia Key Laboratory of Magmatic Mineralization and Ore-Prospecting, Geological Survey of Inner Mongolia, Hohhot 010020, China <juwx1962@163.com>
[5]Department of Geological Sciences, University of Saskatchewan, S7N 5E2 Saskatoon, Saskatchewan, Canada <jim.basinger@usask.ca>

Abstract.—The Silurian and Devonian plant fossil record is the basis for our understanding of the early evolution of land plants, yet our appreciation of early global phytogeographic evolution has been constrained by the focus of most studies on deposits from Europe, North America, and, more recently, South China. Devonian plants have been recorded rarely from northeastern China, and among previous records, few plants have been illustrated and formally described. In this article, megafossil plants representing a Late Devonian-aged (probably Famennian) flora are described from a locality at northern Sonid Zuoqi, Inner Mongolia, NE China. The flora includes *Melvillipteris sonidia* new species, *Archaeopteris* sp., and fragments of some other plants. The new plant shows main axes and two orders of lateral branches. The first-order branches of this plant show a typical zigzag appearance and are borne in pairs on main axes. Second-order branches are straight or slightly flexed, and are borne helically or alternately on first-order branches. Sterile ultimate appendages and fertile structures of *M. sonidia* n. sp. are borne alternately on second-order branches. An associated palynological assemblage, as well as U-Pb ages of detrital zircon grains from adjacent horizons, are also reported, indicating a Late Devonian age in accord with the megafossil plants. The present study contributes to our appreciation of the Devonian floristic diversity of the Xing'an Block, and, through our review of the record of early vascular plants from NE China, more broadly to the understanding of the mid-latitude vegetation of the Northern Hemisphere during the Late Devonian.

Introduction

The colonization of land by early vascular plants has been considered one of the most important evolutionary events in Earth history (Kenrick and Crane, 1997; Taylor et al., 2009), and the Silurian and Devonian fossil record is the major source of evidence for this transformative event. Nevertheless, previous studies have been focused mainly on the records from Europe, North America, and, more recently, South China, with contributions from Gondwana and northwestern China (e.g., Gensel and Andrews, 1984; Anderson et al., 1995; Kenrick and Crane, 1997; Meyer-Berthaud et al., 1999, 2016a, b; Berry et al., 2000; Hammond and Berry, 2005; Gensel, 2008; Taylor et al., 2009; Hao and Xue, 2013; H. Xu et al., 2015; Xue et al., 2018; Prestianni and Gess, 2019), which constrains our understanding of early phytogeographic evolution of land floras.

The vast area of northeastern China was formed through a complex tectonic amalgamation of crustal blocks, including the Erguna Block, Xing'an Block, Songliao-Xilinhot Block, and Jiamusi Block (Fig. 1; Liu et al., 2017). These constitute major components of the eastern part of the Central Asian Orogenic Belt (Sengör et al., 1993). Studies of Devonian plants from these blocks have been limited, with only nine localities reported to contain Late Devonian plant fossils, including the new locality presented herein (Fig. 1.2, localities I–IX; see Discussion for a detailed review). However, only *Leptophloeum rhombicum* Dawson, 1862 from locality VI and two *Archaeopteris* species from locality IX have been illustrated and formally described (IMBG and NIGS, 1974; Cai, 1981); all other reports listed only species names, and the reported fossils are apparently not available for re-investigation.

The recent discovery of a new flora of Late Devonian age from northern Sonid Zuoqi, Inner Mongolia (locality I in Fig. 1.2) presents an opportunity to describe a fossil assemblage, and to review the spatial and stratigraphic distribution of Late Devonian floras from NE China.

Geological setting and stratigraphy

The fossil locality, here called section PM90, is located ~18 km southwest of Dalai Sumu Town, northern Sonid Zuoqi, Inner

*Corresponding authors

https://doi.org/10.1017/jpa.2021.93 Published online by Cambridge University Press

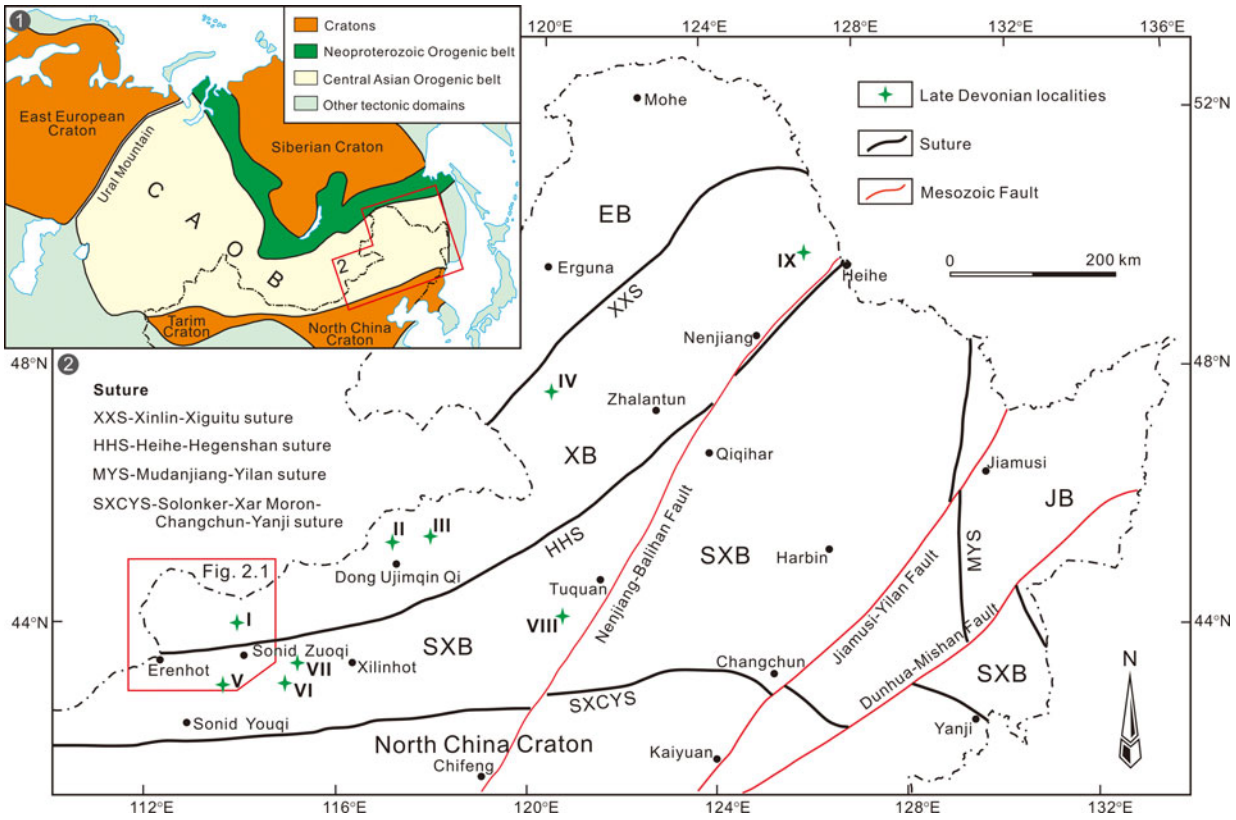


Figure 1. (**1**) Schematic map of Central Asian Orogenic Belt (CAOB) and adjacent tectonic units (modified from Sengör et al., 1993); (**2**) location of Late Devonian plant fossil localities in northeastern China (locality I, this study; localities II-IX, other previous studies). For detailed information about the fossil localities, see Table 3 and the text in Discussion section. The eastern part of the CAOB is composed of several microcontinents and sutures, and here the division scheme of tectonic units proposed by Liu et al. (2017) is followed. Abbreviations of microcontinents: EB, the Erguna Block; XB, the Xing'an Block; SXB, the Songliao-Xilinhot Block; and JB, the Jiamusi Block.

Mongolia, China, and the GPS location is 44°23′25″N, 112° 53′13″E (Fig. 2). A 142-m-thick profile of the plant-bearing succession was measured and divided into 16 beds (PM90 succession for simplicity; Fig. 3). These strata were previously assigned to the upper Carboniferous Hong Obo Formation (IMBG, 1979), or to the upper Carboniferous–lower Permian Baoligaomiao Formation (IMGS, 2007). However, in light of the present discovery of megafossil plants and spores, we conclude that the PM90 succession belongs to the Upper Devonian, which was previously thought to be absent in the Dalai Sumu area. To the south of PM90, sequences with similar lithologies were intruded by Carboniferous-aged granites, or are in fault contact with the brachiopod-bearing Niqiuhe Formation (Early to Middle Devonian-aged marine clastic rocks), while to the north comparable sequences are unconformably overlain by the Baoligaomiao Formation (interbedded clastic and volcanic rocks) (Fig. 2).

The PM90 succession at this time is considered to represent an unnamed lithological unit because it is difficult to compare this succession with any previously recognized unit in the area, where outcrops are usually not well exposed. Nevertheless, a potential candidate for the PM90 succession is the Angeeryin Ul Formation, the stratotype section of which is located near Angeeryin Ul, Dong Ujimqin Qi, Inner Mongolia (locality II in Fig. 1.2), where it is composed of conglomerate, sandstone, siltstone, and mudstone (IMBG, 1973; IMBGMR, 1991, 1996). Based on plant fossils and spores, a Late Devonian age was suggested for the Angeeryin Ul Formation; however, this formation in general is poorly understood. The Angeeryin Ul Formation has been suggested to reach over 4000 m in thickness, yet has been only roughly logged, with single beds varying from tens to hundreds of meters thick (IMBG, 1973; IMBGMR, 1996), and stratigraphic repetition due to tectonic activity has not been fully considered. Thus, at present, it is not possible to precisely compare the PM90 succession with the Angeeryin Ul Formation or indeed any part of it.

Four lithological facies are recognized in the PM90 succession. Facies *Gm* consists of pebble-supported, massive conglomerate, gray in color, and occurring only in bed-7 (Fig. 4.1); it typically occurs as units ranging from 1.5–2 m in thickness, with graded bedding. Sub-rounded cobbles up to 20 mm long are poorly sorted and are mainly lithic fragments (~50%) or quartz (~30%). Siltstone, tuff, andesite, granite porphyry, and mudstone constitute the lithic fragments, indicating low compositional maturity. An erosional surface and imbrications are evident at the base of bed-7 (Fig. 4.1), with dip angles of the imbrications ~15–30°. Gravels are irregularly distributed in bed-7, and lenses of sandstone are interbedded within the gravels of the *Gm* facies. The *Gm* facies are interpreted as representing channel lag deposits, in light of the massive coarse sediments, erosional surfaces, and imbricate structure (Allen, 1964; Miall, 1977; Makaske, 2001; Tucker, 2003; Nichols, 2009).

https://doi.org/10.1017/jpa.2021.93 Published online by Cambridge University Press

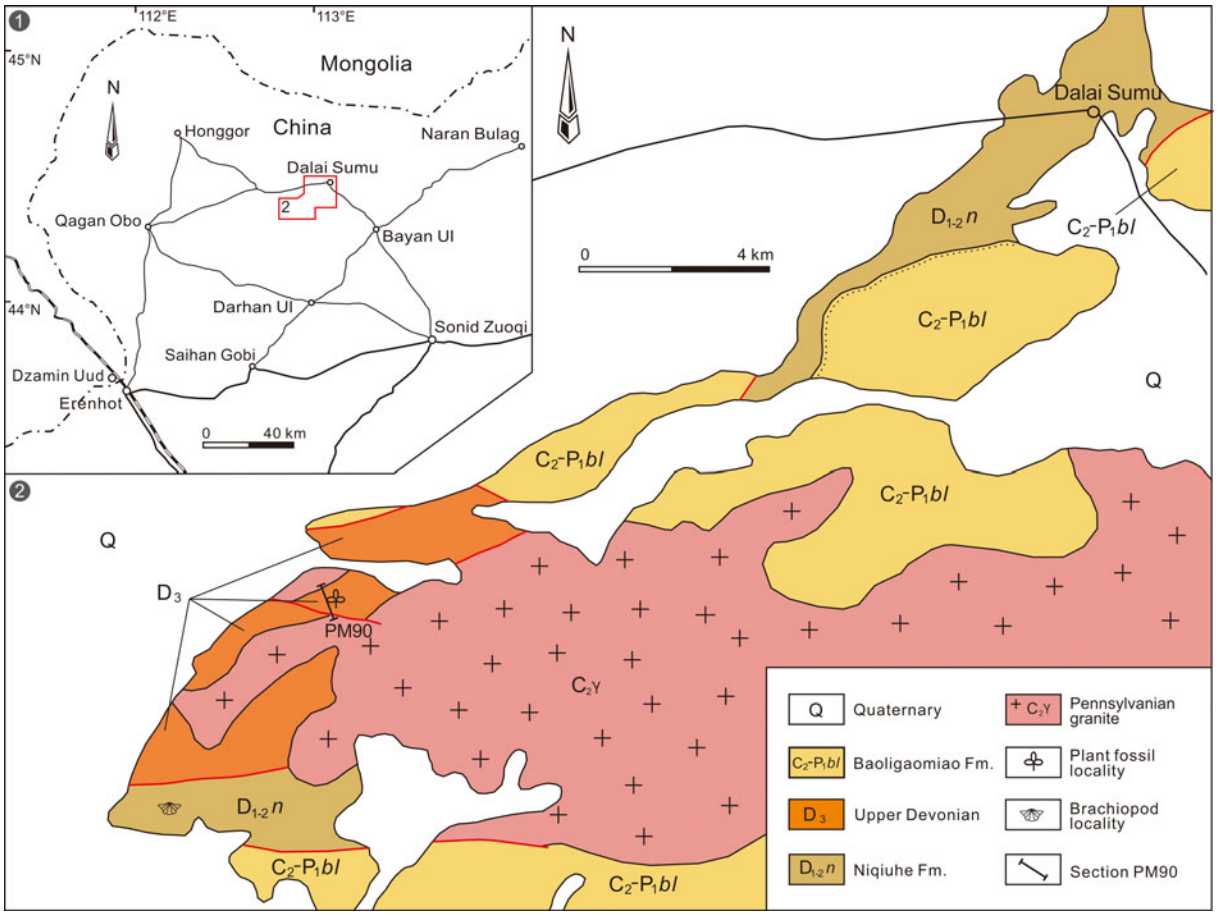


Figure 2. (**1**) Map showing the location of the studied area. (**2**) Geological sketch map (modified from IMGS, 2007) showing the location of the studied section (PM90) and geologic setting near Dalai Sumu, Sonid Zuoqi, Inner Mongolia, NE China.

Facies *Sp* is a thinly to thickly bedded sandstone, with individual units ranging from 4 cm to 1 m in thickness, and cumulative thickness of >51 m (bed-1 to bed-6). Graded bedding and planar cross-bedding occur (Fig. 4.2, 4.3), with cross-bed dip angles ~20–30°. The grains are sub-rounded, poorly to moderately sorted, fine- to coarse-grained sand, and rare gravel (Fig. 5.1). The lithology is lithic wacke or feldspathic wacke (sensu Pettijohn, 1975), containing quartz (20–35%), feldspar (5–30%), and lithic fragments (30–70%) (Fig. 5.2). Facies *Sp* is interpreted as point-bar deposits in a fluvial setting, in that graded bedding and planar cross-bedding are generally found in such lateral-accretion deposits (Allen, 1964; Miall, 1977; Makaske, 2001; Tucker, 2003).

Facies *Fl* is composed of gray to dark-gray laminated (thinly bedded) siltstone, with rare sandstone lenses (Fig. 4.6). The grains are dominantly silt (70–75%), with some clay (25–30%) and rare fine-grained sand (5%). Thickness of beds ranges from 2 mm to 10 cm, and the cumulative thickness can reach up to 37 m. Horizontal bedding is common (Fig. 4.5), with laminae formed by variation in content of silt grains (Fig. 5.3), and the beds may be rich in plant fossils (bed-12). Facies *Fl* is interpreted as representing vertical-accretion deposits formed in a floodplain environment through overbank flooding (Allen, 1964; Nanson and Croke, 1992; Makaske, 2001; Gradziński et al., 2003; Nichols, 2009).

Facies *Fm* is composed of massive mudstone (Fig. 5.4), devoid of visible bedding (Fig. 4.4), with a gray-green, but sometimes mottled red color. Plant fossils are found in abundance in some parts of the bed (Fig. 4.7). Like facies *Fl*, facies *Fm* is interpreted as representing vertical-accretion deposits in a floodplain environment, where plant remains were deposited near their growth site (Allen, 1964; Nanson and Croke, 1992; Makaske, 2001; Gradziński et al., 2003).

The PM90 succession includes sandstone at the base (bed-1 to bed-6; Cycle I), followed by three complete fining-upwards cycles (Cycles II–IV) (Table 1). The basal sandstone may represent an incomplete fining-upward cycle, but much has been lost due to erosion and deposition of the overlying conglomerate. Cycle II (bed-7 to bed-12) forms the main part of the section and is 81.7 m in overall thickness, including imbricated conglomerate with erosional surface at the base (facies *Gm*), sandstone with graded- and cross- bedding (facies *Sp*) in the lower part, and thick fines with abundant plant debris in the upper part (facies *Fl* and *Fm*). Cycles such as this typically develop in a fluvial environment: facies *Gm* is interpreted as a lag deposit; *Sp*, lateral point-bars; and *Fl* and *Fm*, overbank floodplain deposits (Allen, 1964; Miall, 1977; Makaske, 2001; Tucker, 2003; Bridge, 2006; Nichols, 2009). The third and fourth cycles are thinner, probably representing sediments of a lower energy environment, perhaps ephemeral rivers. Sediments

https://doi.org/10.1017/jpa.2021.93 Published online by Cambridge University Press

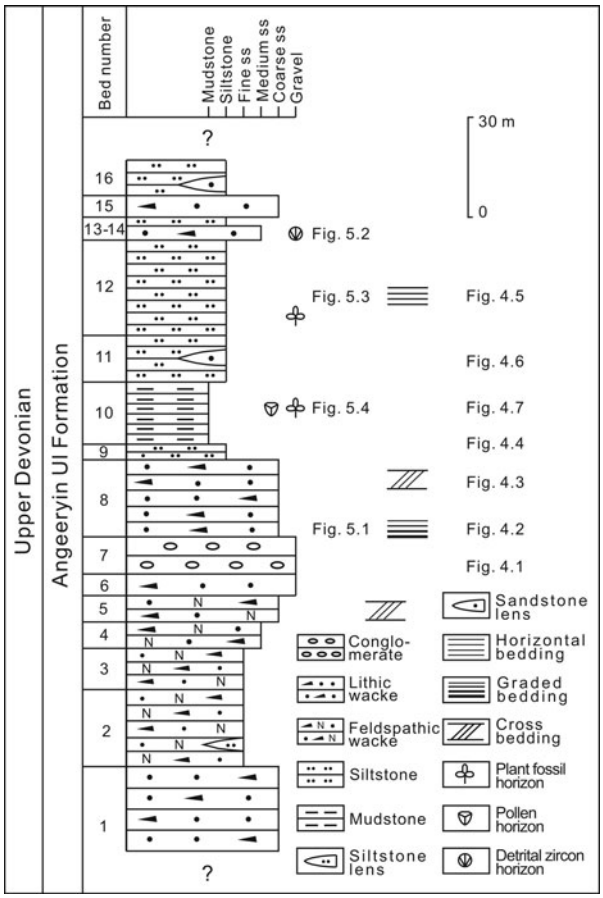


Figure 3. Stratigraphic column of section PM90, showing the source of megafossil plants, palynomorphs, and detrital zircon sample. The sedimentary features and representative rocks are shown in Figures 4 and 5.

throughout the section are interpreted as having been deposited close to their provenance, given the immature nature of the conglomerate and sandstone.

Material and methods

Plant megafossils were obtained from bed-10 and bed-12 of the section PM90 (Fig. 3). Hundreds of specimens of a new euphyllophyte plant (Figs. 6–12) were recovered from both beds. A few specimens of *Archaeopteris* (Figs. 13, 14) were collected from bed-10, and a possible sphenophyllalean plant and some unidentified axes and roots (Fig. 15) were collected from bed-12. All specimens are preserved as adpressions in siltstone or mudstone.

Some specimens were treated by acetic acid (2 mol/L) solution to remove surface carbonate film and to enhance contrast between plant axes and the surrounding rock matrix. The fossils were prepared by dégagement with steel needles to better expose morphology, and were photographed with a digital camera.

One palynological sample collected from bed-10 was treated using standard HCl-HF acid maceration at the Nanjing Institute of Geology and Palaeontology, Chinese Academy of Sciences (NIGPAS). The rock fragments were processed in 30% HCl, followed by decant washing in water to neutralize and then demineralization in 60% HF with repeated stirring. Organic matter from the residues was then mounted and the recognized palynomorphs photographed.

One sample of lithic wacke (PM90TW13) from bed-13 was collected for detrital zircon U-Pb dating, using Laser Ablation-Multicollector-Inductively Coupled Plasma-Mass Spectrometry (LA-MC-ICP-MS) at the Inner Mongolia Key Laboratory of Magmatic Mineralization and Ore-prospecting, China. The methodology and data of zircon U-Pb dating are available at Dryad (http://datadryad.org/; https://doi.org/10.5061/dryad.d51c5b042).

Repositories and institutional abbreviations.—Types and other megafossil specimens examined in this study are deposited in the Geological Museum, School of Earth and Space Sciences, Peking University (PKU), Beijing, China. All slides of palynomorphs are deposited at NIGPAS.

Systematic paleobotany

Phylum Tracheophyta Sinnott, 1935 ex Cavalier-Smith, 1998
Subphylum Euphyllophytina Kenrick and Crane, 1997
Order Rhacophytales Taylor et al., 2009
Family Incertae sedis
Genus *Melvillipteris* Xue and Basinger, 2016

Type species.—*Melvillipteris quadriseriata* Xue and Basinger, 2016, by original designation, from the Parry Islands Formation (Famennian), Upper Devonian, eastern Melville Island, Canadian Arctic Archipelago.

Diagnosis.—See Xue and Basinger (2016, p. 603).

Melvillipteris sonidia Bai, Huang, Basinger, and Xue, new species
Figures 6–12

Holotype.—PKUB18801a (Fig. 7.1), from the Late Devonian of northern Sonid Zuoqi, Inner Mongolia, northeastern China.

Paratypes.—PKUB18810c, 18814, 18816, 18821a, 18830, 18857b, 18860a, 18861a, and 18874b (Figs. 6.1, 6.6, 7.4, 9.2, 9.7, 9.8, 10.1, 10.7, 12.1).

Diagnosis.—Main axes bent slightly or moderately, ~3.5 (2.0–6.6) mm wide and at least 215 mm long, with internode length ~80 mm. First-order branches with a swollen base, inserted on main axes in pairs. First-order branches with a zigzag appearance, ~2.1 (1.0–3.8) mm wide and up to at least 108 mm long, bending at each node at angles of ~139° (125–147°). Second-order branches ~1.0 (0.5–2.5) mm wide and up to at least 95 mm long, borne helically or alternately, departing from first-order branches at angles of ~102° (82–122°), with internode length 14–46 mm, and bearing alternate to sub-opposite ultimate appendages that may be fertile or sterile. Sterile ultimate appendages inserted alternately on second-order branches, with internode length 4.0–39 mm, with two or three successive dichotomies and paired recurved tips, ~0.5 mm wide at the proximal portion, up to ~6.8 mm in

https://doi.org/10.1017/jpa.2021.93 Published online by Cambridge University Press

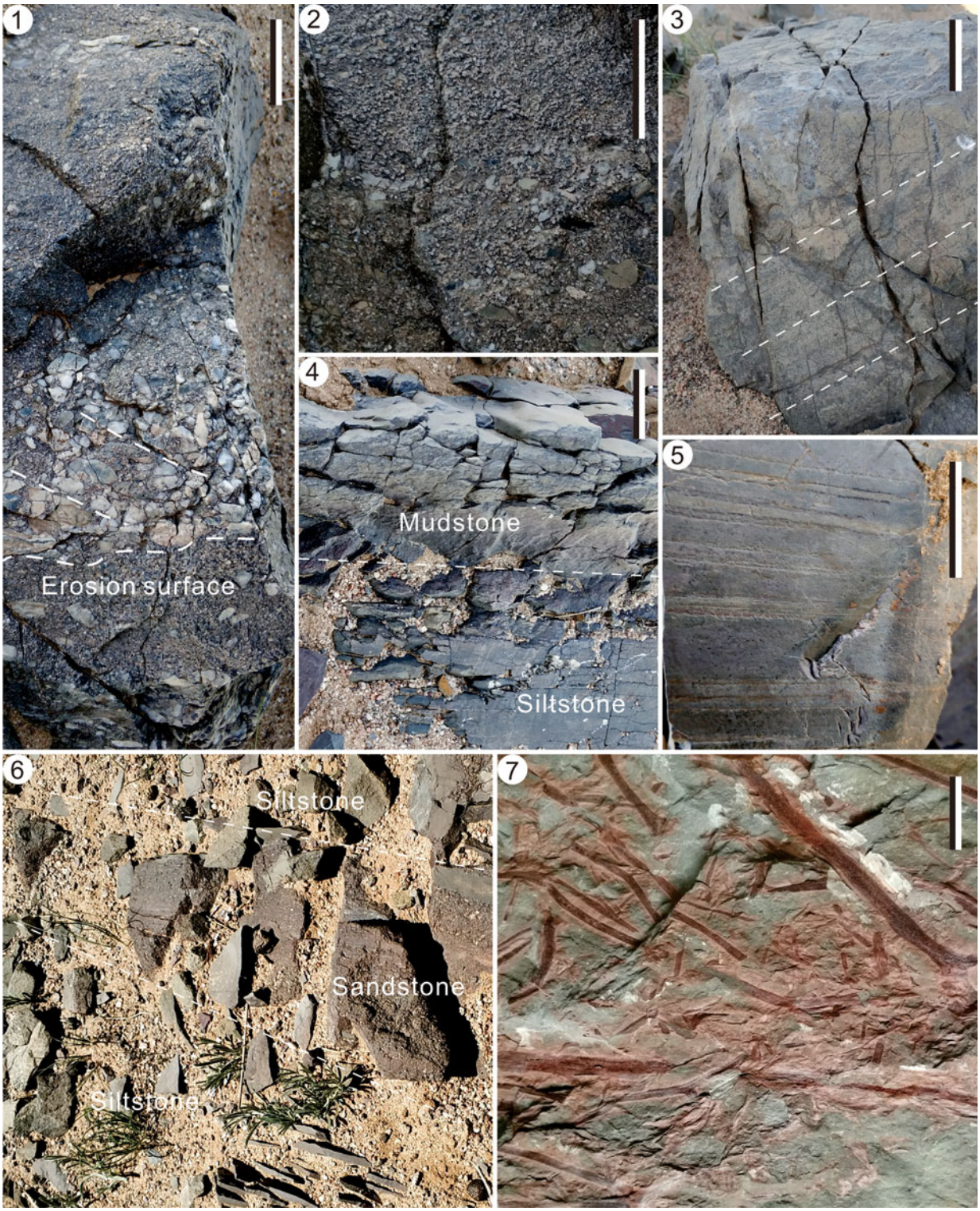


Figure 4. Sedimentary features at section PM90. (**1**) Conglomerate with erosion surface and imbrication at the base (bed-7); (**2**) gravelly coarse-grained sandstone with graded bedding (bed-8); (**3**) coarse-grained sandstone with planar cross-bedding (bed-8); (**4**) gradational contact between bed-9, siltstone with laminations (lower part of the photo), and bed-10, massive mudstone (upper part); (**5**) siltstone with horizontal bedding (bed-12); (**6**) siltstone, containing a lens of sandstone (bed-11); (**7**) mudstone with abundant plant fossils (bed-10). Scale bars = 20 mm.

overall length. Each fertile structure with a short stalk ~2.3 (1.4–3.8) mm long and an initial dichotomy forming two sister branches, each of which supports a sporangial cluster. Each sporangial cluster branched dichotomously two or three times, with six or more terminal sporangia. Sporangia fusiform, borne singly or in pairs on ultimate divisions, ~1.3 (0.8–1.9) mm in length and ~0.4 (0.2–0.7) mm in maximum width.

https://doi.org/10.1017/jpa.2021.93 Published online by Cambridge University Press

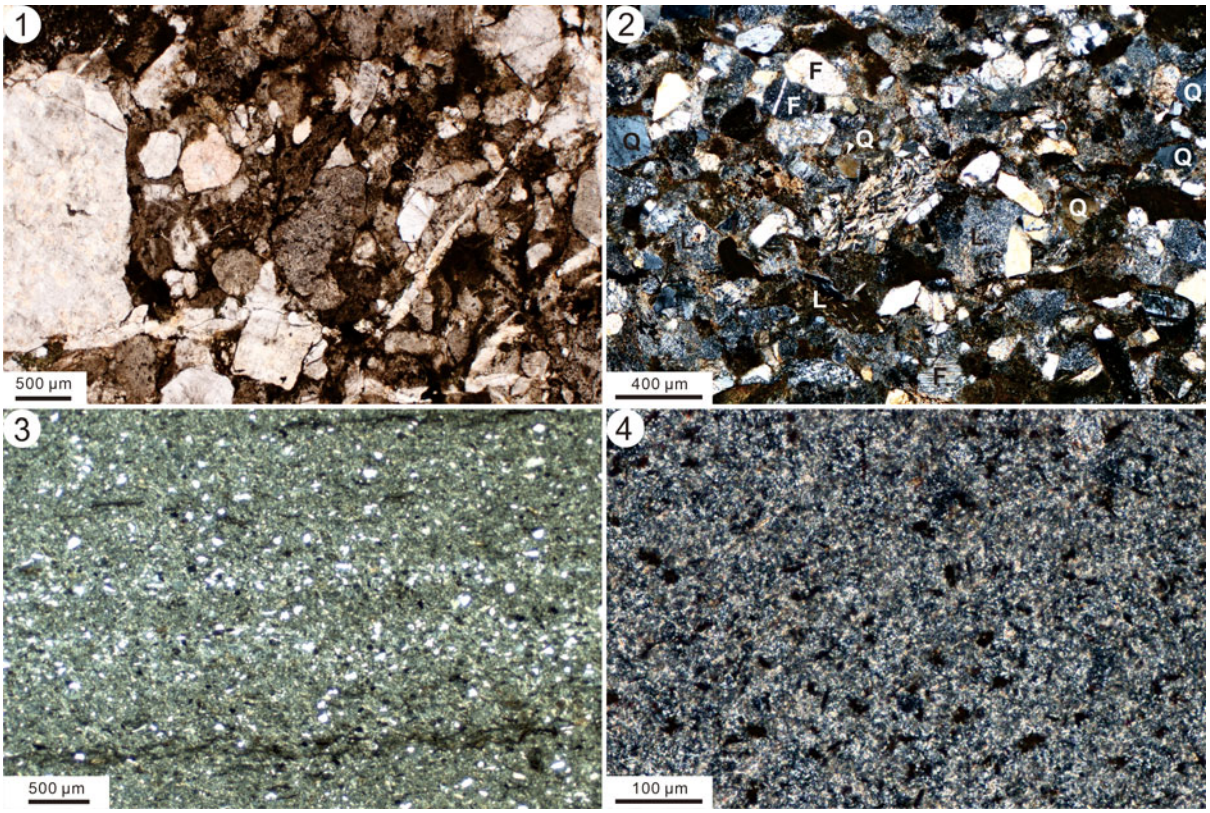


Figure 5. Photomicrographs of main rock types from section PM90. (**1**) Lithic wacke (bed-8), showing poorly sorted grains; (**2**) lithic wacke (bed-13); (**3**) siltstone in vertical profile (bed-12) showing horizontal lamination; (**4**) mudstone (bed-10). Q, quartz; F, feldspar; L, lithic fragments.

Occurrence.—Upper Devonian, an unnamed lithological unit, 18 km southwest of Dalai Sumu Town, northern Sonid Zuoqi, Inner Mongolia, China (GPS location: 44°23′25″N, 112° 53′13″E).

Description.—

Main axes.—Orders of branching are distinguished by size, morphology, arrangement of lateral organs, and organic connections. The most robust axes are interpreted as main axes, although this interpretation is tentative because no roots have been found. Main axes show different preservation status. (1) They clearly show a pair of first-order branches at the nodes of some main axes (Figs. 6.1 upper node, 6.2, 8). (2) In some cases, one of the first-order branches is usually well preserved or exposed, while the other one is represented by a broken base (Fig. 6.3, 6.4) or is demonstrated to extend into the rock matrix (Fig. 6.6, 6.7). (3) Some main axes appear to bear one only lateral branch at the node (Fig. 6.5), but we consider that, in these cases, the second of a pair of branches is either unexposed or has been broken off during preservation. (4) In some specimens, a main axis bears a pair of first-order branches, but above the node the distal part of main axis may appear to be missing (Figs. 6.8, 6.9, 7.1, 7.3), although distal remains of the axis may be recovered through careful dégagement (Fig. 7.4, 7.5). In all cases, the first-order branches show a swollen base, a criterion for distinguishing them from second-order branches.

Main axes are bent slightly to moderately at the nodes where first-order branches depart, and are straight or nearly so between the nodes (Fig. 6.1–6.7). The diameter of main axes ranges from 2.0–6.6 mm, average 3.5 mm (N = 16; Fig. 11), with the width decreasing when approaching the branching point. The longest preserved main axis is 21.5 cm long, with two nodes bearing first-order branches, and shows an interval of ~8.0 cm between the nodes (Fig. 6.1). A fertile structure has been found attached to a probable main axis (Fig. 6.11).

First- and second-order branches.—First-order branches have been found attached to their main axes (Figs. 6–8), while many others are detached (Fig. 9). First-order branches show a consistent morphology: they have a swollen base and are bent at each node where a second-order axis departs, such that the bending angles of 125–147°, with an average of 139° (N = 14), creates a characteristic zigzag appearance (Figs. 7.1, 9.1–9.4, 9.10, 9.11). First-order branches range from 1.0–3.8 mm in width, average 2.1 mm (N = 39; Fig. 11), but the swollen base is much wider, reaching up to ~9.1 mm wide, and the most proximal portion of a first-order branch may exceed 4.0 mm in diameter, as for example in Figure 7.1. The longest preserved first-order branch is 10.8 cm in length, without showing taper. A fertile structure has been found on a probable first-order branch (Fig. 7.1 arrow f1, 7.2).

Second-order branches found attached to first-order branches appear to be arranged alternately, although this also could be attributed to a helical pattern; presently there is insufficient evidence to distinguish between these two patterns. Second-order branches depart from first-order branches at an average angle of 102° (range = 82–122°, N = 13), and the interval between two successive second-order branches ranges from 14.2–45.7 mm (average = 27.4 mm, N = 6).

https://doi.org/10.1017/jpa.2021.93 Published online by Cambridge University Press

Table 1. Lithological descriptions of the plant-bearing succession at section PM90 (see Fig. 3 for the logged column). *Bed thickness is uncertain because of heavy cover. Abbreviation of facies codes: *Gm* = massive conglomerate; *Sp* = sandstone with or without cross-bedding; *Fl* = laminated siltstone; *Fm* = massive mudstone.

Bed no.	Thickness (m)	Color	Texture	Sedimentary structures	Rock type	Facies	Fining-upward cycles
16	?*	Dark-gray	Silt-dominated	Thinly bedded, with lenses of sandstone	Siltstone	*Fl*	IV
15	5.4	Dark-gray	Medium- to coarse-grained sand-dominated, with gravels; sub-rounded; poorly sorted; grain-supported	Medium bedded	Lithic wacke	*Sp*	
14	2.4	Dark-gray	Silt-dominated	Thinly bedded	Siltstone	*Fl*	III
13	1.5	Gray-green	Fine- to medium-grained sand-dominated; sub-rounded; moderate sorted; grain-supported	Medium-bedded	Lithic wacke	*Sp*	
12	25.3	Gray	Silt-dominated	Thinly bedded; horizontal bedding; bearing plant fossils	Siltstone	*Fl*	II
11	12.0	Dark-gray	Silt-dominated	Thinly bedded, with lenses of sandstone	Siltstone	*Fl*	
10	14.3	Gray-green	Clay-dominated	Massive; bearing abundant plant fossils	Mudstone	*Fm*	
9	3.6	Gray	Silt-dominated	Thinly bedded	Siltstone	*Fl*	
8	17.9	Gray-green	Varied-grained sand-dominated; sub-rounded; poorly sorted; grain-supported	Medium-bedded; graded bedding at lower part; cross-bedding at upper part	Lithic wacke	*Sp*	
7	8.6	Gray	Gravel-dominated, with sand; sub-rounded; poorly sorted; pebble-supported	Massive; with erosion surface and imbrication at base; pebbles unevenly distributed; with lenses of sandstone	Conglomerate	*Gm*	
6	5.5	Gray-green	Varied-grained sand-dominated; sub-rounded; poorly sorted; grain-supported	Medium-bedded	Lithic wacke	*Sp*	I
5	7.0	Gray-green	Medium- to coarse-grained sand-dominated; sub-rounded; moderate sorted; grain-supported	Medium-bedded, with cross-bedding	Lithic wacke	*Sp*	
4	7.0	Gray-green	Medium-grained sand-dominated; sub-rounded; moderate sorted; grain-supported	Medium-bedded	Lithic wacke	*Sp*	
3	7.0	Gray-green	Fine-grained sand-dominated; sub-rounded; moderate sorted; grain-supported	Thinly bedded	Feldspathic wacke	*Sp*	
2	24.5	Gray-black	Fine-grained sand-dominated; sub-rounded; moderate sorted; grain-supported	Thinly bedded, with lenses of siltstone	Feldspathic wacke	*Sp*	
1	?*	Gray-green	Medium- to coarse-grained sand-dominated; sub-rounded; moderate sorted; grain-supported	Thickly bedded	Lithic wacke	*Sp*	

Second-order branches are slender and straight to slightly flexed in appearance (Figs. 9.5, 9.8, 10.1–10.4), with a width of 0.5–2.5 mm (average = 1.0 mm, N = 34; Fig. 11). The longest preserved second-order axis is 95 mm long (Fig. 10.1). Second-order branches appear to terminate in a series of anisotomies in quick succession (Fig. 10.5). Lateral organs are attached to the second-order branches in an alternate to subopposite pattern (Fig. 10.1–10.3, white dots), and may be sterile ultimate appendages (Fig. 10.4 arrows U) or fertile structures (Fig. 10.1–10.3, 10.6, 10.7 arrows f). The interval between appendages along the second-order branches ranges from 4.0–38.6 mm (average = 20.2 mm, N = 7).

Sterile ultimate appendages (SUAs).—In only two specimens, ultimate appendages that are probably sterile are found attached to the base of first-order branches, but they are very poorly preserved, with only a short, undivided fragment left (Fig. 6.6–6.10). Numerous other first-order branches show no evidence of SUAs.

SUAs regularly occur on second-order branches, but most are incomplete. In the specimen shown in Figure 10.8, a SUA departs from its parent axis at a right angle, extends ~4.3 mm, and then divides once (dichotomy I); one of the daughter branches extends into rock matrix, while the other daughter branch extends ~1.8 mm and then further divides (dichotomy II); the dichotomy II produces a sharply recurved tip ~1.3 mm long, while its sister tip runs into matrix. SUAs shown in Figure 10.9 and 10.10 are similar, but show a third dichotomy: their initial dichotomy (dichotomy I) produces two daughter branches, the first branch is partially buried in the matrix or has been broken off, and the second is visible and shows further divisions (dichotomies II and III); of the two daughter branches produced by dichotomy II, one is either incomplete or lies buried within the matrix, and a second isotomously divides once (dichotomy III) and produces two terminal divisions with oppositely recurved tips. It is clear that the branching of the SUAs is three-dimensional. The specimen in Figure 10.11 shows two overlapped, incomplete SUAs; compared with the SUA in Figure 10.10, the left one may represent dichotomy II of a SUA, while the right one represents an ultimate dichotomy (dichotomy III) with two recurved tips. Other SUAs show consistent branching patterns (e.g., Fig. 10.12). Thus, the features of SUAs of second-order branches can be summarized as follows: they divide two or three times, with a branching angle of 70–140°, forming a three-dimensional, dichotomous branching system, and are terminated in oppositely recurved tips. In overall length,

https://doi.org/10.1017/jpa.2021.93 Published online by Cambridge University Press

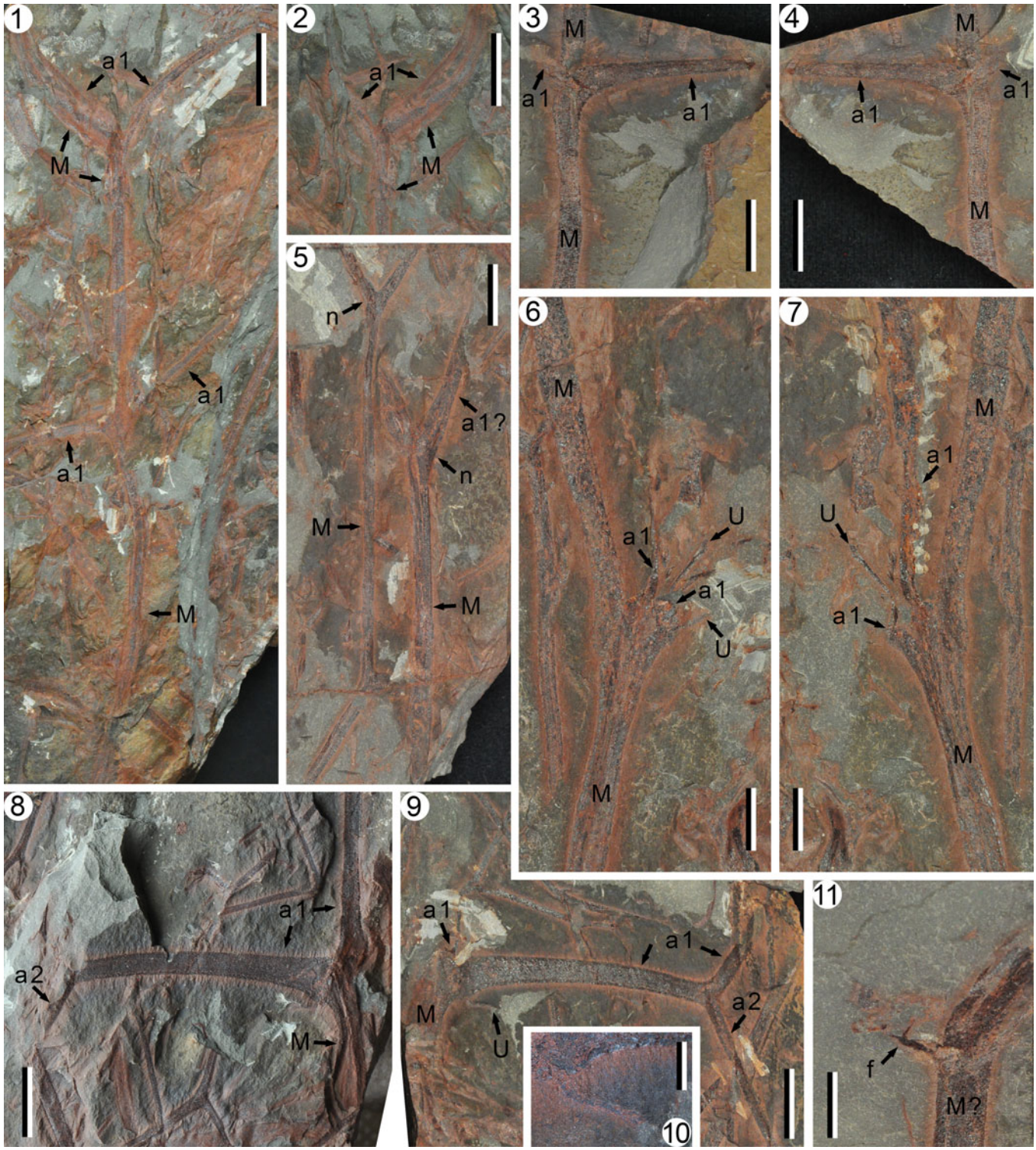


Figure 6. *Melvillipteris sonidia* n. sp. (**1**) Main axis; the upper node shows a pair of first-order branches, and immediately below this node is a bend of the main axis; in the middle, a node shows another pair of first-order branches; the axes show little contrast with the surrounding matrix, and thus a interpretative line drawing is presented in Figure 8; paratype, PKUB18861a; (**2**) counterpart of the upper node of the main axis in (**1**); PKUB18861b; (**3, 4**) part and counterpart; main axis with a pair of first-order branches, one of which is represented by a broken base; PKUB18859a, b; (**5**) two main axes with lateral branches; note that the nodal position is expanded (arrows n); PKUB18854b; (**6, 7**) part and counterpart; main axis with a pair of first-order branches; one branch is well preserved, and the other branch extends into the rock matrix; broken ultimate appendages occur at the base of a branch; paratype PKUB18860a, PKUB18860b; (**8, 9**) part and counterpart; main axis and two first-order branches; one branch shows a swollen base with a broken ultimate appendage (arrow U) and a second-order branch, distally; PKUB18873a, b; (**10**) enlargement of the broken ultimate appendage in (**9**, arrow U); (**11**) fertile structure attached to a probable main axis; sporangia can be confirmed on higher magnification; PKUB18865. M = main axis; a1 = first-order branch; a2 = second-order branch; U = sterile ultimate appendage; f = fertile structure. Scale bars: (**1, 2**) 20 mm; (**3–5, 8–9**) 10 mm; (**6–7, 11**) 5 mm; (**10**) 2 mm.

https://doi.org/10.1017/jpa.2021.93 Published online by Cambridge University Press

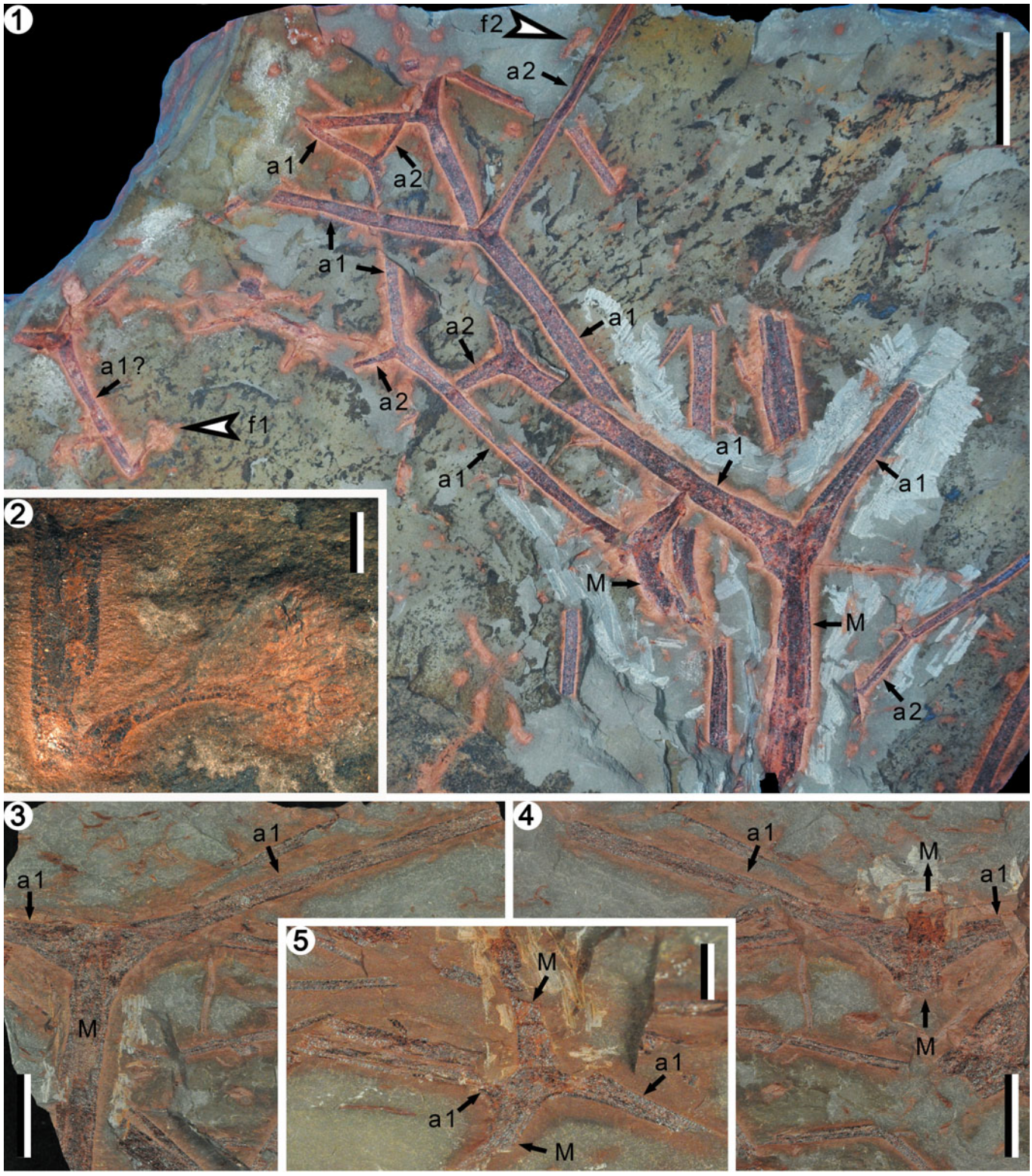


Figure 7. *Melvillipteris sonidia* n. sp. (**1**) Holotype; specimen showing main axes and two orders of lateral branches; arrows f1 and f2 indicate two fertile structures enlarged in (**2**) and Figure 12.2, respectively; the right main axis bears a pair of first-order branches; the distal part of this main axis is missing above the node; PKUB18801a; (**2**) fertile structure (f1 in **1**) attached to a probable first-order branch with a long stalk; (**3, 4**) part and counterpart; PKUB18857a and paratype, 18857b; main axis and pair of first-order branches; distal part of the main axis above the node is missing in (**3**), but has been revealed through dégagement in (**4**); (**5**) main axis and pair of first-order branches; PKUB18876. M = main axis; a1 = first-order branch; a2 = second-order branch; f = fertile structure. Scale bars: (**1**) 20 mm; (**2**) 2 mm; (**3, 4**) 10 mm; (**5**) 5 mm.

https://doi.org/10.1017/jpa.2021.93 Published online by Cambridge University Press

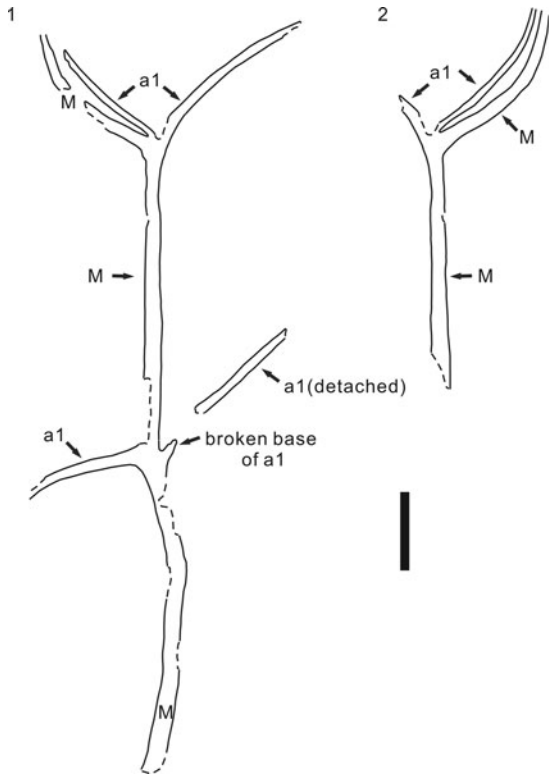


Figure 8. Interpretative drawings of a main axis and its first-order branches of *Melvillipteris sonidia* n. sp. (**1, 2**) Part and counterpart of the specimen shown in Figure 6.1 and 6.2. M = main axis; a1 = first-order branch. Scale bar: 20 mm.

these SUAs reach up to 6.8 mm and at the base are ~0.5 mm wide. The tips (ultimate divisions) are short, 0.5–1.3 mm long, sharply recurved, and tapering.

Fertile structures.—Most fertile structures are detached from their axes. One fertile structure has been found attached to what may be a main axis (Fig. 6.11, based on its larger width), and another one to a first-order branch (Fig. 7.1 arrow f1, 7.2), but these are rare occurrences, and it may be that the interpretation of their parent axes as main axis or first-order branch is incorrect. Nevertheless, one specimen shows a fertile structure at the branching point of a first-order branch (Fig. 9.7), and a second specimen shows a fertile structure very close to the branching point of a first-order branch (Fig. 9.6). We interpret these as fertile structures borne at the base of second-order branches. More commonly, however, fertile structures are found attached along the length of second-order branches at an acute to right angle (Figs. 9.8, 9.9, 10.1–10.3, 10.6, 10.7).

Fertile structures are dichotomously branched. Each fertile structure extends 1.4–3.8 mm (average = 2.3 mm, N = 7) to form a short, straight stalk (Figs. 9.9, 10.6, 10.7), with a width of 0.6–0.9 mm (average = 0.7 mm, N = 8). This stalk then divides dichotomously at an angle of 70–120° to form daughter branches 0.3–0.6 mm in width (average = 0.4 mm, N = 15) and 0.8–1.5 mm in length (average = 1.1 mm, N = 6). Subsequent dichotomies occur at shorter intervals, making this initial dichotomy more conspicuous and forming a pair of sporangial clusters (Fig. 12.1, 12.9), which themselves consist of two or more trusses of sporangia.

The fertile specimen shown in Figure 12.1 is the best preserved. The stalk of this fertile structure initially dichotomizes to form the branches S1 and S1′ that support the two sporangial clusters. The branch S1 then divides to support two fertile trusses, each of which consists of at least three sporangia. The branch S1′ also supports two fertile trusses: one composed of at least four sporangia (sporangia 7–10 in Fig. 12.1), the other with at least three sporangia (sporangia 11–13 in Fig. 12.1). In some specimens, numerous sporangia are densely compressed together (Fig. 12.2), and in some others, fertile structures are only partially preserved (Fig. 12.3–12.7). In the specimen shown in Figure 12.8, the right sporangial cluster shows at least seven sporangia. In the specimen shown in Figure 12.9, the left sporangial cluster, similarly, contains two fertile trusses, each with at least four sporangia. Many other specimens show only part of a complete fertile structure, such as one of the two sporangial clusters (Fig. 12.3), or simply a fertile truss with several sporangia (Fig. 12.4, 12.5, 12.7). The entire fertile structure consists of two sporangial clusters, collectively with 12–16 sporangia. The sporangia are borne singly (e.g., Fig. 12.1 sporangia 3 and 11), or in pairs (Fig. 12.1, 12.4, 12.5, 12.7), on terminal divisions.

The sporangia are fusiform in shape, 0.8–1.9 mm long (average = 1.3 mm, N = 61) and 0.2–0.7 mm in maximum width (average = 0.4 mm, N = 61), and with a pointed tip. A dehiscence line was not observed due to poor preservation. No *in situ* spores were found.

Etymology.—From Sonid Zuoqi, where the plant was collected.

Remarks.—Our material is assigned to the genus *Melvillipteris* as a new species, *M. sonidia* n. sp. This genus was established from the Late Devonian (Famennian) of Arctic Canada (Xue and Basinger, 2016). The similarities between *M. sonidia* n. sp. and the type species, *M. quadriseriata*, are striking (Table 2): both plants show main axes with paired first-order branches; their first-order branches show a swollen base, and in rare cases bear ultimate appendages on the base, although in both plants this structure has been poorly preserved; in both, sterile ultimate appendages and fertile structures are alternately arranged along the second-order branches; their sterile ultimate appendages are terminated in oppositely recurved tips; their fertile structures are similar in showing a two-clustered appearance, and each sporangial cluster dichotomizes two to three times, with sporangia borne singly or in pairs on terminal divisions; in addition, quantitatively, the measurements of main axes, first- and second-order branches, sterile ultimate appendages, and fertile structures are quite similar between the Inner Mongolian plant and *M. quadriseriata* (Table 2). In the new plant, we are not able to demonstrate how the paired first-order branches are arranged on main axes because most main axes are preserved in fragments. Given the above numerous similarities, however, a quadriseriate arrangement, as in *M. quadriseriata*, can be inferred in *M. sonidia* n. sp. (i.e., pairs of first-order branches are alternately arranged along the main axes).

The differences between *M. sonidia* n. sp. and *M. quadriseriata* are also notable: first-order branches of *M. quadriseriata* are straight and bear sterile ultimate appendages in the proximal

https://doi.org/10.1017/jpa.2021.93 Published online by Cambridge University Press

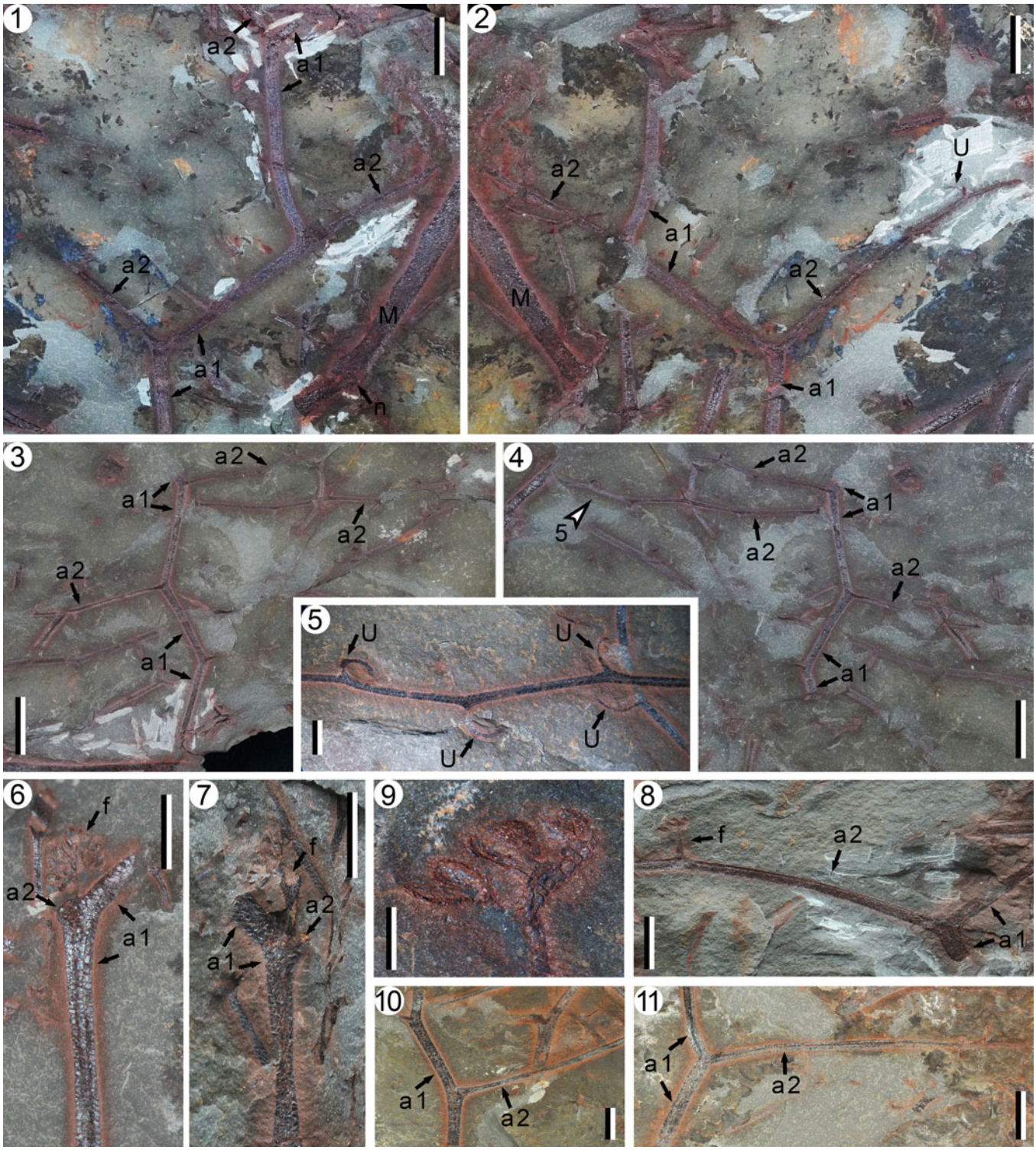
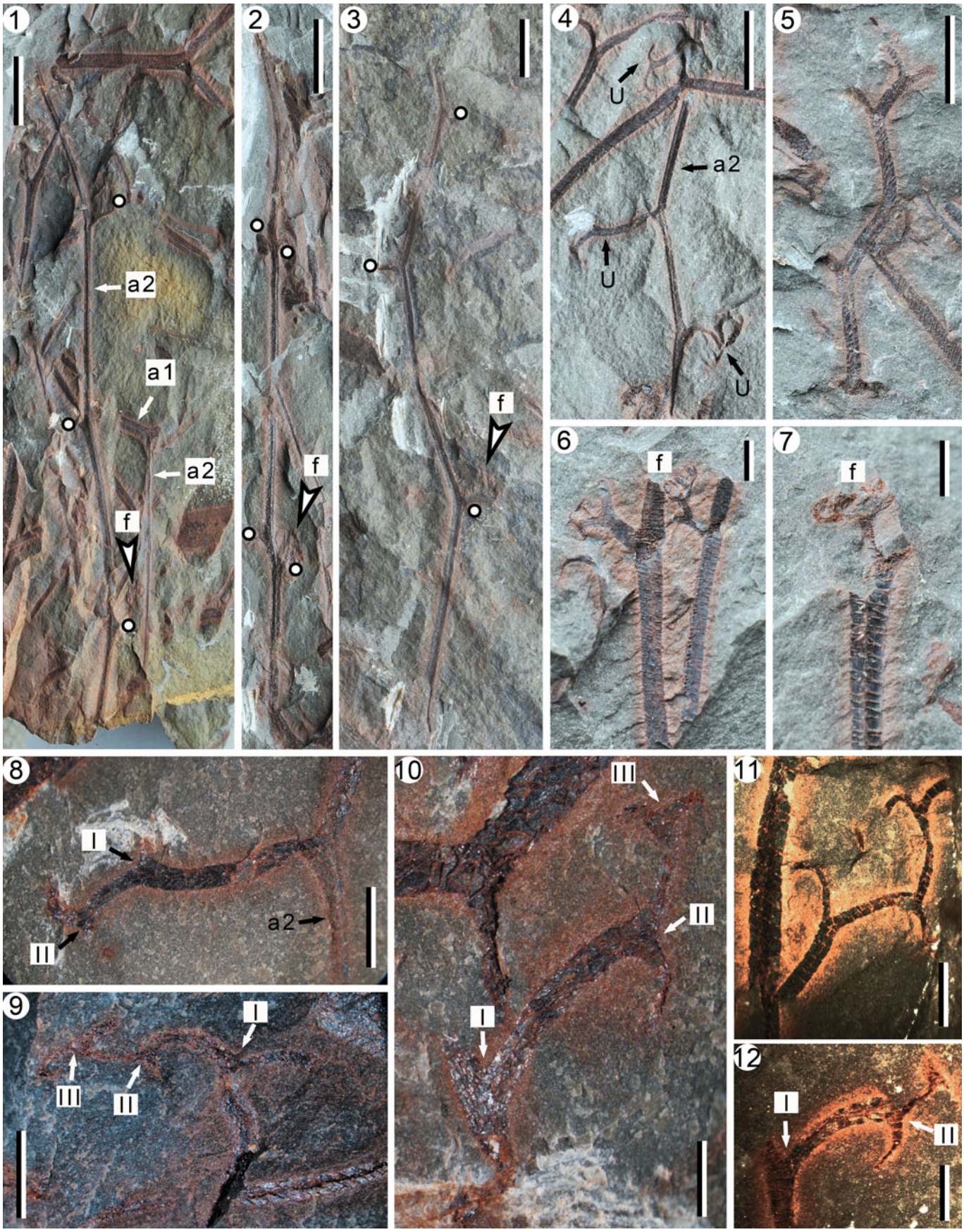


Figure 9. *Melvillipteris sonidia* n. sp. (**1, 2**) Part and counterpart; PKUB18874a, 18874b, paratype; zigzag first-order branch with second-order branches; also showing main axis with expanded nodal position (arrow n); (**3, 4**) part and counterpart; PKUB18862a, c; first-order branch and second-order branches; arrow 5 points to the part enlarged in (**5**); (**5**) enlargement of second-order branch with sterile ultimate appendages; PKUB18862c; (**6**) first-order branch, and a fertile structure close to the branching point; PKUB18810b; (**7**) first-order branch, and a fertile structure attached at the branching point; a second-order branch demonstrated by its broken base; paratype PKUB18810c; (**8**) first-order branch with a second-order branch, the latter bearing a fertile structure; paratype PKUB18814; (**9**) enlargement of the fertile structure in (**8**); (**10, 11**) first-order branches with their second-order branches; (**10**) PKUB18858a; (**11**) PKUB18869b. M = main axis; a1 = first-order branch; a2 = second-order branch; U = sterile ultimate appendage; f = fertile structure. Scale bars: (**1–4**) 10 mm; (**5**) 2 mm; (**6–8, 10, 11**) 5 mm; (**9**) 1 mm.

https://doi.org/10.1017/jpa.2021.93 Published online by Cambridge University Press



https://doi.org/10.1017/jpa.2021.93 Published online by Cambridge University Press

Figure 10. *Melvillipteris sonidia* n. sp. (**1**) Second-order branches, one of which bears alternate laterals (white dots); paratype PKUB18816; (**2**) second-order branch, with alternate to sub-opposite laterals (white dots); PKUB18814-2; (**3**) second-order branch, with alternate laterals (white dots); PKUB18832; arrows f (**1–3**) indicate poorly preserved fertile structures, confirmed on higher magnification; (**4**) second-order branch and sterile ultimate appendages; PKUB18812b-1; (**5**) terminal part of a second-order branch; PKUB18821a-1; (**6**) second-order branch bearing ultimate appendages or fertile structures; PKUB18812b-2; (**7**) fertile structure attached to a second-order branch; paratype PKUB18821a-2; (**8**) enlargement of a sterile ultimate appendage (shown in **4**, middle arrow U) composed of a twice dichotomously branching system (arrows I and II); (**9, 10**) incomplete sterile ultimate appendages, which are dichotomously branched three times (arrows I to III); (**9**) PKUB18875; (**10**) PKUB18812b-1; (**11**) two overlapped, incomplete ultimate appendages; the right one with terminal, recurved tips; PKUB18812a-2; (**12**) ultimate appendage, dichotomously branched twice (arrows I and II) and with terminal, recurved tips; PKUB18821a-3. M = main axis; a1 = first-order branch; a2 = second-order branch; U = sterile ultimate appendage; f = fertile structure. Scale bars: (**1**, **2**) 10 mm; (**3–5**) 5 mm; (**6–9, 11**) 2 mm; (**10**, **12**) 1 mm.

portions, but those of *M. sonidia* n. sp. are typically zigzag and bear no appendages in the proximal portions; sterile ultimate appendages of second-order branches dichotomize once or twice in *M. quadriseriata*, but dichotomize two or three times in *M. sonidia* n. sp.; in *M. quadriseriata*, each sporangial cluster of a fertile structure is supported by a long, recurved branch, while in *M. sonidia* n. sp., the two sporangial clusters extend in the same direction and are not recurved.

Xue and Basinger (2016) provided detailed comparisons between *Melvillipteris* and other related plants, particularly those with quadriseriate branching, and tentatively assigned this genus to the Rhacophytales (sensu Taylor et al., 2009). Their comparisons remain valid and applicable to *M. sonidia* n. sp. Besides *Melvillipteris*, many other plant genera (e.g., *Rhacophyton* Crépin; *Cephalopteris* Nathorst; *Protocephalopteris* Ananiev; *Ellesmeris* Hill, Scheckler, and Basinger; *Chlidanophyton* Gensel; *Eocladoxylon* Koidzumi; *Protopteridophyton* Li and Hsü) were collectively included in the Rhacophytales (Hilton, 1999; Berry and Wang, 2006; Taylor et al., 2009), and the quadriseriate branching in these taxa may be a shared derived character (synapomorphy) (Xue and Basinger, 2016). However, taxonomic assignment of *Melvillipteris* to the Rhacophytales remains uncertain and requires further phylogenetic analyses. First, the lack of anatomy for *Melvillipteris* hinders a comparison with the well-studied genus *Rhacophyton*, which shows a clepsydroid-shaped strand of primary xylem surrounded by secondary xylem (Leclercq, 1951; Andrews and Phillips, 1968). Second, the arrangement of fertile structures in *Melvillipteris* along second-order branches differs from the fertile structures of *Rhacophyton*, which are borne at the base of lateral branches, occupying a catadromic position (Leclercq, 1951; Andrews and Phillips, 1968), and fertile structures of *Cephalopteris* and *Protocephalopteris* are borne at a similar position (Ananiev, 1960; Schweitzer, 1968). Nevertheless, some specimens in *M. sonidia* n. sp. appear to show fertile structures at the base of second-order branches (e.g., Fig. 9.6, 9.7), which could be considered a possible equivalent of the catadromic fertile structures in *Rhacophyton* and other members of the Rhacophytales. Studies based on additional materials are needed to resolve the phylogenetic position of *Melvillipteris* and plants collectively assigned to the Rhacophytales.

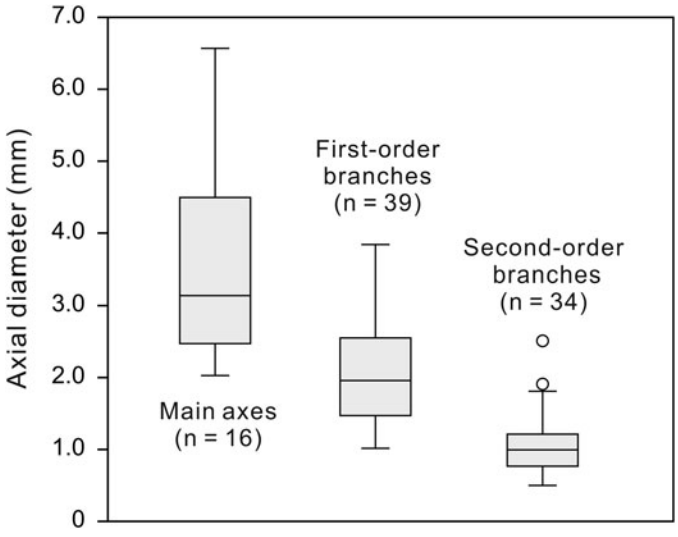


Figure 11. Box plot of the measured width of main axes, first-, and second-order branches. For each order of axis: the 25–75% quartiles of the measurements are drawn using a box; the median value, a horizontal line inside the box; and the minimal and maximum values, short horizontal line below and above the box. Circles represent some extreme values of the measured width of second-order branches.

Class Progymnospermopsida Beck, 1960
Order Archaeopteridales Zimmermann, 1930
Family Archaeopteridaceae Schmalhausen, 1894
Genus *Archaeopteris* (Dawson, 1871) Stur, 1875

Type species.—*Archaeopteris hibernica* (Forbes, 1853) Stur, 1875, by original designation.

Archaeopteris sp.
Figures 13, 14

Description.—One slab shows ultimate branches and scattered leaves (Fig. 13.1). Five complete leaves are obovate in shape, 14.6–17.1 mm in length and 4.4–5.8 mm in maximum width, and possess a crenulate to entire distal margin (Fig. 13.2, 13.8). One of the ultimate branches, ~0.6 mm wide and ~19 mm long, bears multiple leaves along one only side, while other leaves are not preserved (Fig. 13.8).

Specimen PKUB18802a and its counterpart show a penultimate branch and laterals (Figs. 13.3–13.7, 14). The penultimate branch is incomplete, ~2.4 mm wide and ~89 mm long, with broken ends, and bears at least five lateral organs that depart at an acute angle of 30–40° (Figs. 13.3, 14 letters a–e). While most laterals are poorly preserved, one clearly represents a leafy ultimate branch (Figs. 13.3 arrow b = UB, 14 lateral b = UB). The ultimate branch is curved downward, ~0.8 mm wide and ~66 mm in preserved length, with distal parts absent. At least 17 leaves can be observed along this ultimate branch (Figs. 13.5, 13.6, 14.2 numerals 1–17). These leaves are densely packed, making it difficult to determine the arrangement. Some

https://doi.org/10.1017/jpa.2021.93 Published online by Cambridge University Press

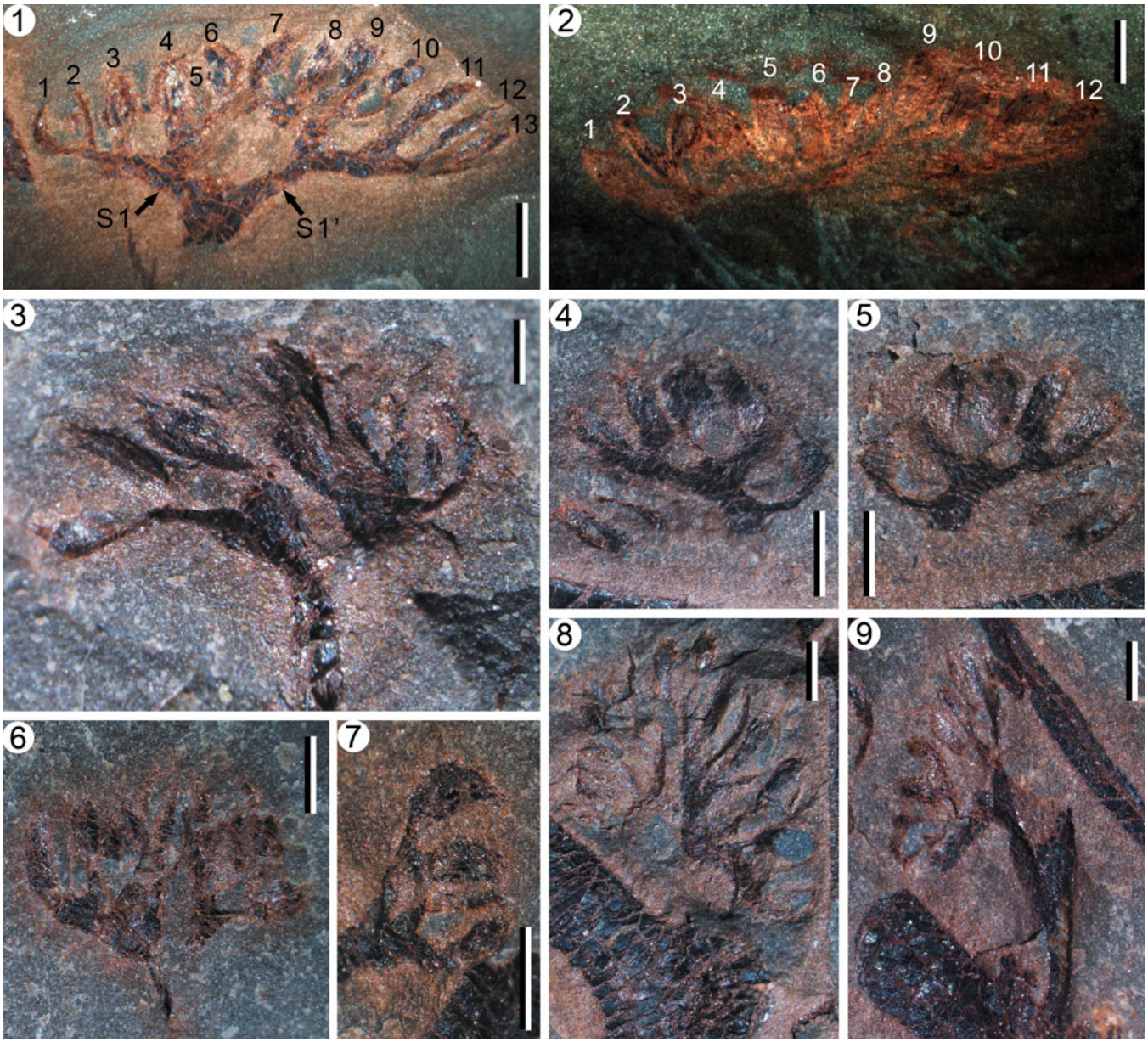


Figure 12. *Melvillipteris sonidia* n. sp. (**1–9**) Fertile structures: (**1**) fertile structure showing an initial dichotomy, two major sporangial clusters supported by branches S1 and S1′, and 13 sporangia (numerals 1–13); paratype PKUB18830; (**2**) fertile structure enlarged from Figure 7.1 (arrow f2), showing at least 12 sporangia (numerals 1–12); (**3**) incomplete fertile structure; PKUB18812c; (**4**, **5**) incomplete fertile structure, showing paired sporangia on terminal divisions; part and counterpart, PKUB18821a-4, 18821b-4; (**6**) fertile structure with two sporangial clusters; PKUB18812a-4; (**7**) incomplete fertile structure, showing terminal, paired sporangia; PKUB18812a-2; (**8**) fertile structure with two sporangial clusters, the right cluster better preserved; enlarged from the counterpart of the specimen in Figure 9.6 (arrow f); PKUB18810a; (**9**) incomplete fertile structure, showing one of the sporangial clusters; enlarged from Figure 9.7 (arrow f). Scale bars: (**1–9**) 1 mm.

leaves appear to lie beneath the branch (Fig. 14.2 leaves 4, 7, 8, 12, 17), while others lie on the upper surface of the branch (Fig. 14.2 leaves 1, 2, 5, 9, 13). It is neither possible to distinguish between adaxial and abaxial surfaces of leaves, nor possible to demonstrate whether there is leaf dimorphism. Distal margins of most leaves are incomplete, but one leaf shows that the distal margin is shallowly dissected (Fig. 13.7), although this is considered to be a preservational artifact (compare Fig. 13.2, 13.7, 13.8). More complete leaves are obovate in shape, depart at an angle of 35–48°, appear sessile with no distinct petiole, and are 12.5–15.8 mm long and 4.8–5.4 mm in maximum width. Venation appears to be open dichotomous.

Remarks.—Specimens are assignable to the genus *Archaeopteris* based on gross leaf and branch morphology. *Archaeopteris* was an important component of global Late Devonian floras (Fairon-Demaret et al., 2001; Guo and Wang, 2009; Taylor et al., 2009), and has been reconstructed as a tall tree (Meyer-Berthaud et al., 1999). Leaves in this genus show great variation in morphology. Our specimens are distinct from those with deeply dissected leaves (e.g., *A. fissilis*

https://doi.org/10.1017/jpa.2021.93 Published online by Cambridge University Press

Table 2. Morphological comparisons between *Melvillipteris quadriseriata* and *M. sonidia* n. sp. Data for *M. quadriseriata* based on Xue and Basinger (2016). All measurements are in mm.

Species	*Melvillipteris quadriseriata*	*Melvillipteris sonidia* n. sp.
Locality	Melville Island, Nunavut, Canadian Arctic Archipelago	Dalai Sumu Town, northern Sonid Zuoqi, Inner Mongolia, China
Main axis		
Morphology	zigzag to straight	slightly or moderately bent
Width	3.0–6.0	2.0–6.6
Internode length	20–60	~80
First-order branch		
Morphology	paired; with a swollen base; straight	paired; with a swollen base; zigzag
Width	0.9–2.5	1.0–3.8
Internode length	12–22	14.2–45.7
Second-order branch		
Width	~0.7	0.5–2.5
Internode length	3.1–16.6	4.0–38.6
Sterile ultimate appendage of second-order branch		
Arrangement	alternate	alternate
Divisions	1–2	2–3
Overall length	4.0–5.3	up to 6.8
Ultimate division	recurved; length: 0.7–1.9	recurved; length: 0.5–1.3
Fertile structure		
Morphology	comprised of two sporangial clusters, which are oppositely recurved	comprised of two sporangial clusters, which extend in the same direction
Divisions	3–4	3–4
Stalk (proximal portion before the first dichotomy)	width: 0.3–0.7; length: 1.7–4.0	width: 0.6–0.9; length: 1.4–3.8
Number of sporangia	≥12	≥12
Sporangium		
Shape	fusiform	fusiform
Size	maximum width: 0.3–0.5; length: 1.0–1.4	maximum width: 0.2–0.7; length: 0.8–1.9

Schmalhausen, 1894, *A. macilenta* Lesquereux, 1884, and *A. notosaria* Anderson, Hiller, and Gess, 1995), but similar with those with crenulate to entire margins (e.g., *A. halliana* [Göppert, 1859] Stur, 1875 = *A. roemeriana* [Göppert, 1859] sensu Stockmans, 1948) (Kenrick and Fairon-Demaret, 1991; Anderson et al., 1995; Fairon-Demaret et al., 2001; Taylor et al., 2009). The shallow dissection in some of our leaves appears to be a result of poor preservation.

Among the species of *Archaeopteris*, our plant is most similar to *A. halliana*. As in our specimens, the leaves of *A. halliana* usually have been described as entire, while some show crenulate margins (e.g., Fairon-Demaret and Leponce, 2001, figs. 3, 12). Leaves of our specimens, ~15 mm long and ~5 mm in maximum width, fit well within the range of leaves of *A. halliana* from Belgium (Fairon-Demaret and Leponce, 2001, based on >350 leaves). Anisophylly as an essential character is demonstrated in *A. halliana* (i.e., an ultimate branch bears both smaller and larger leaves) (Fairon-Demaret and Leponce, 2001), although it is not possible to demonstrate this character in our specimens due to poor preservation. Thus, it is appropriate to treat our specimens as *Archaeopteris* sp.

Archaeopteris has been previously reported from two other localities of the Xing'an Block, or more broadly, NE China. The first record is from the Angeeryin Ul Formation near Zhunsaber, Dong Ujimqin Qi, Inner Mongolia (Fig. 1.2, Table 3, locality III; IMBG, 1976); however, there is no description or illustration available for a comparison with our specimens. Cai (1981) described two species of *Archaeopteris* (*A.* cf. *A. sphenophyllifolia* Lesquereux, 1884, and *Archaeopteris* sp.) from the Xiaohelihe Formation at a locality near Handaqi, Heihe, Heilongjiang Province (Fig. 1.2, Table 3, locality IX). Cai's first species shows deeply dissected leaves, which is quite different from our specimens. His second species is poorly preserved, with leaves of similar shape and size as in our specimens, but distal margins of the leaves are unclear.

A possible sphenophyllalean plant
Figure 15.1–15.4

Description.—This plant is poorly preserved and the fossils show very low contrast with the surrounding rock matrix. Leaves that can be recognized in the first specimen (Fig. 15.1, 15.2) apparently are arranged in a whorl, but are highly overlapped; one leaf is wedge-shaped, at least 16 mm long, and shows open dichotomous venation (Fig. 15.3). Dégagement of this specimen shows that the leaf remains occupy a circular area that is ~37 mm in diameter and can be clearly distinguished from the surrounding matrix (Fig. 15.2), indicating the outline of a leaf whorl. The second specimen also shows a wedge-shaped leaf ~16 mm long (Fig. 15.4). Leaf veins indicate that the leaves are flabellate.

Remarks.—Plants in the order Sphenophyllales constitute an important component in the Paleozoic floras, spanning the Late Devonian to late Permian (Batenburg, 1982; Wang et al., 2005, 2006; Bashforth and Zodrow, 2007; Xiong and Wang, 2008; Taylor et al., 2009; Prestianni and Gess, 2019). Slender axes with nodes and internodes, and linear, spatulate, or wedge-shaped leaves borne in whorls, are key shared characters (Galtier and Daviero, 1999; Bashforth and Zodrow, 2007; P. Huang et al., 2018). Our material is potentially assignable to the Sphenophyllales, in the presence of wedge-shaped leaves that apparently are arranged in a whorl. Our plant differs from species with linear, or deeply dissected,

https://doi.org/10.1017/jpa.2021.93 Published online by Cambridge University Press

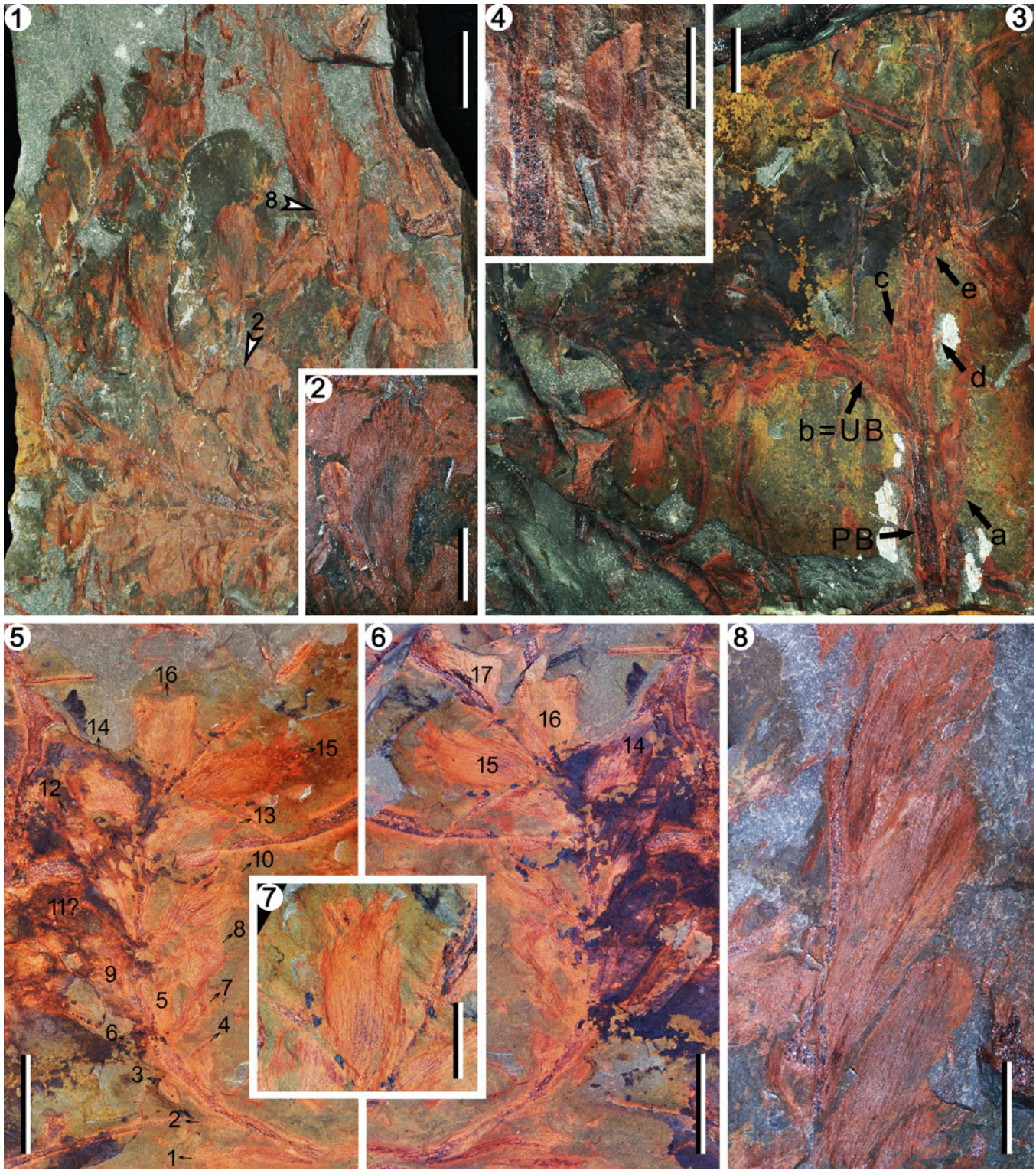


Figure 13. *Archaeopteris* sp. (**1**) Slab with ultimate branches and scattered leaves; arrow 2 points to the leaf enlarged in (**2**); arrow 8 points to the part enlarged in (**8**); PKUB18888a; (**2**) enlargement of a leaf showing serrate margin; (**3**) penultimate branch with an ultimate branch (arrow b = UB); other laterals (arrows a, c–e) can be recognized by their broken bases; see line drawing in Figure 14.1; PKUB18802a; (**4**) enlargement of lateral a in (**3**), a partially preserved leaf; (**5, 6**) part and counterpart, enlargement of the ultimate branch shown in (**3**), with at least 17 leaves (numerals 1–17); leaf 15 in (**6**) is enlarged in (**7**); see line drawing in Figure 14.2; PKUB18802a, b; (**7**) enlargement of a leaf; dissection of its distal margin may be a preservational artifact; (**8**) leaves attached on ultimate branch. Scale bars: (**1**, **3**, **5, 6**) 10 mm; (**2, 4, 7, 8**) 5 mm.

https://doi.org/10.1017/jpa.2021.93 Published online by Cambridge University Press

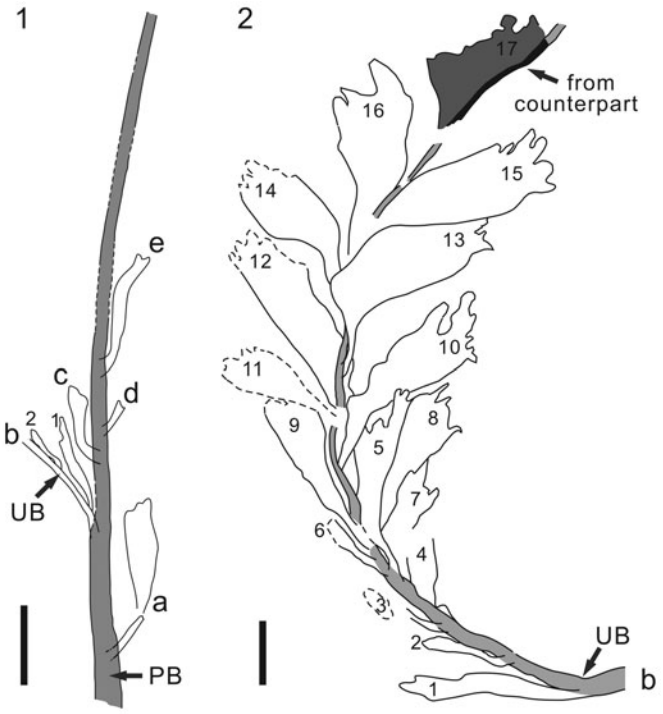


Figure 14. Interpretative line drawings of *Archaeopteris* sp. (**1**) Penultimate branch (arrow PB), based on the specimen shown in Figure 13.3, with at least five lateral organs (a–e); only very proximal portions of lateral b, with two leaves, shown (numerals 1, 2) (complete drawing of this lateral is shown in **2**); (**2**) ultimate branch and leaves, based on the specimen shown in Figure 13.5, with leaf 17 from the counterpart shown in Figure 13.6. Labels for the laterals and leaves same as in Figure 13.3–13.6. Leaf venation is poorly preserved in most leaves, and thus is not shown. Scale bars: (**1**) 10 mm; (**2**) 5 mm.

or lobed leaves, such as *Hamatophyton verticillatum* Gu and Zhi, 1974; *Rinistachya hilleri* Prestianni and Gess, 2019; *Rotafolia songziensis* (Feng, 1984) Wang et al., 2005; *Sphenophyllum oblongifolium* (Germar and Kaulfuss, 1831) Unger, 1850; *S. pseudotenerrimum* Sze, 1936; *S. changxingense* Huang et al., 2018; and others (Galtier and Daviero, 1999; Wang et al., 2005, 2006; Deng et al., 2016; P. Huang et al., 2018; Prestianni and Gess, 2019), while similar wedge-shaped, unlobed leaves occur in the Late Devonian species *S. lungtanense* Gothan and Sze, 1933 (Wang et al., 2008).

Axes and roots of indeterminate plants
Figure 15.5, 15.6

Description.—Axes of unknown plants are found within the beds (Fig. 15.5, 15.6). One of the axes reaches ~40 mm in width, indicating it is a part of a large-bodied plant (Fig. 15.5). Several adventitious roots, ~2.2 mm wide, are attached as a cluster to one side of an axis (Fig. 15.6, upper axis).

Remarks.—These axes and roots cannot be assigned to any known taxon, and they are shown here only for the purpose of documentation.

Spores

The sample from bed-10 mainly yielded miospores (Fig. 16), which are in low abundance and in poor to moderate preservation. The recognized taxa include: *Ambitisporites dilutes* (Hoffmeister, 1959) Richardson and Lister, 1969; *Ambitisporites* sp.; *Aneurospora* sp.; *Apiculiretusispora* spp.; *Cymbosporites conatus* Bharadwaj et al., 1971; *Cymbosporites cyathus* Allen, 1965; *Densosporites* sp.; *Dibolisporites* sp.; *Gulisporites hiatus* Lu, 1997; *Gulisporites intropunctatus* Lu, 1981; *Gulisporites* spp.; *Lophotriletes* sp.; *Lycospora* sp.; *Reticulatisporites* sp.; and *Retusotriletes* sp. Most cannot be identified at the species level with certainty. Additionally, there are some indeterminable spores and rare acritarchs.

Discussion

Age of the flora.—Megafossil plants from the PM90 succession include *Melvillipteris sonidia* n. sp., *Archaeopteris* sp., a possible sphenophyllalean plant, and fragments of other plants. The type species of *Melvillipteris* has been reported from the Late Devonian (Famennian) Parry Islands Formation of Melville Island, Canadian Arctic Archipelago (Fig. 17; Xue and Basinger, 2016). The genus *Archaeopteris* has a worldwide distribution, mostly reported from the Upper Devonian of South China, North America, Europe, Morocco, Australia, South Africa, and Colombia (Fig. 17; Beck, 1960; Hao and Mei, 1987; Beck and Wight, 1988; Anderson et al., 1995; Cai and Wang, 1995; Meyer-Berthaud et al., 1999; Berry et al., 2000; Guo and Wang, 2009, 2011; Orlova et al., 2016), although there are also some Middle Devonian occurrences (Berry and Fairon-Demaret, 2001). *Archaeopteris* apparently became extinct at about the Devonian-Carboniferous boundary, and rare reports from the earliest Carboniferous remain to be verified (Fairon-Demaret, 1986; Scheckler, 1986). Based on data essentially from Laurasia, seven floral assemblage zones were established by Banks (1980) for the interval from the late Silurian to earliest Carboniferous. The *Archaeopteris* Zone, marked by the appearance of *Archaeopteris*, was said to be Late Devonian (Frasnian and Famennian) in age, above which is the *Rhacophyton* Zone with an age of latest Devonian to earliest Carboniferous (Banks, 1980; Fairon-Demaret, 1986; Scheckler, 1986). However, the development of provincialism may hinder the application of such biozonations outside of Laurasia (Edwards and Berry, 1991). Nevertheless, by combining the evidence of megafossil plants (the co-occurrence of *Melvillipteris* and *Archaeopteris*), spores, and U-Pb ages of detrital zircons, the PM90 succession is suggested to be Late Devonian, and most probably Famennian, in age.

Spores from the PM90 succession, although only preliminarily reported herein, also suggest a Late Devonian age. While *Cymbosporites cyathus* was first reported from the Middle Devonian (Givetian) of Vestspitsbergen (Allen, 1965), this species commonly occurs in the Late Devonian of South China (Ouyang et al., 2017), and in the basal part of the Heishantou Formation (around the Devonian-Carboniferous boundary) in Xinjiang, northwestern China (Lu, 1999). *Cymbosporites conatus* shows a similar temporal distribution as the type species, also with a record from the basal Heishantou Formation of Xinjiang (Lu, 1999; Ouyang et al., 2017). *Gulisporites intropunctatus* was described from the lower Upper Devonian of Sichuan, and *Gulisporites hiatus*, from the Famennian Shaodong Formation of Hunan, South China (Lu, 1981, 1997). Regionally, previous

https://doi.org/10.1017/jpa.2021.93 Published online by Cambridge University Press

Table 3. List of macrofossil plants and spores from the Late Devonian deposits of northeastern China. *Locality numbers, same as in Figure 1.2. **Taxa with published illustrations are indicated in **bold**; all other taxa have been neither illustrated nor described in previous reports. ***Plant fossils occur only in the lower part of the Seribayan Obo Formation, while marine fossils of early Mississippian age occur in the upper part (IMBGMR, 1991, 1996).

*Locality number	Lithological units	Location	**Reported taxa	References
I	Unnamed unit (Late Devonian)	Dalai Sumu, Sonid Zuoqi, Inner Mongolia	***Melvillipteris sonidia* n. sp.; *Archaeopteris* sp.; and numerous spore taxa (see text)**	This study
II	Angeeryin Ul Formation (Late Devonian)	Angeeryin Ul, Dong Ujimqin Qi, Inner Mongolia	*Lepidodendropsis* sp. Spores: *Reticulatisporites* sp.; *Ancyrospora* sp.; *Leiotriletes* sp.; *Granulatisporites* sp.; *Acanthotriletes* sp.	IMBG, 1973
III	Angeeryin Ul Formation (Late Devonian)	Zhunsaber, Dong Ujimqin Qi, Inner Mongolia	*Archaeopteris* sp.; *Aneurophyton* sp.; *Knorria* sp.; Spores: *Ancyrospora* sp.	IMBG, 1976
IV	Angeeryin Ul Formation (Late Devonian)	Bugetu, Ewenkizu Zizhiqi, Heilongjiang	*Lepidodendropsis cyclostigmatoides* Jongmans et al., 1937; *Sublepidodendron* sp.; *Protocephalopteris* sp.; *Moresnetia zalesskyi* Stockmans, 1948; *M.* (*Lenlogia*) *krishtofovchii*, Petrosyan in Lepekhina et al., 1962	HLJBG, 1981
V	***Seribayan Obo Formation (Late Devonian–early Mississippian)	Seribayan Obo, Sonid Zuoqi, Inner Mongolia	*Leptophloeum rhombicum*	IMBG, 1965
VI	***Seribayan Obo Formation (Late Devonian–early Mississippian)	Qiqigeyin Obo, Abag Qi, Inner Mongolia	***Leptophloeum rhombicum*** (Illustrated in IMBG and NIGS, 1974, Plate 203-9, 9a)	IMBG, 1974; IMBG and NIGS, 1974
VII	***Seribayan Obo Formation (Late Devonian–early Mississippian)	Gun Nur, Abag Qi, Inner Mongolia	*Leptophloeum rhombicum*; *Archaeocalamites* sp.	IMBG, 1974
VIII	***Seribayan Obo Formation (Late Devonian–early Mississippian)	Tagetatu, Jarud Qi, Inner Mongolia	*Archaeocalamites* sp.	Wang et al., 2012
IX	Xiaohelihe Formation (Late Devonian)	Handaqi, Heihe, Heilongjiang	***Archaeopteris* cf. *A. sphenophyllifolia*** (Illustrated in Cai, 1981, Plate I-8); ***Archaeopteris* sp.** (Illustrated in Cai, 1981, Plate I-9, 10); *Sublepidodendron* sp.; *Sphenopteris* sp.; *Knorria* sp.	Cai, 1981; Xue et al., 1982

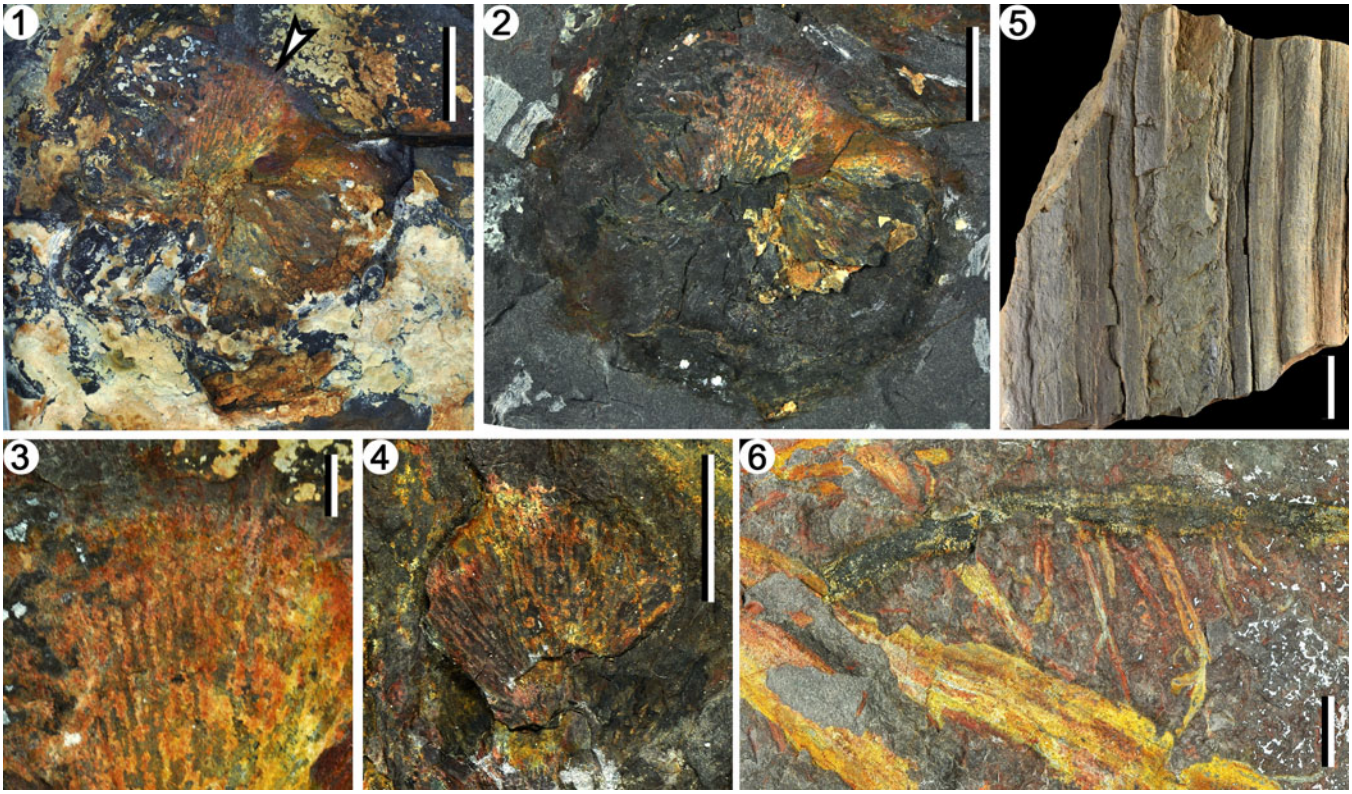


Figure 15. Other plants. (**1–4**) A possible sphenophyllalean plant: (**1**) a whorl of many leaves, which are highly overlapped, and are partially covered and surrounded by white carbonate materials; arrow points to the best preserved leaf enlarged in (**3**); PKUB18803-2; (**2**) dégagement stage of the specimen in (**1**), after removal of carbonate materials; a circular outline is shown, indicating the trace of a leaf whorl; (**3**) enlargement of distal part of a leaf shown in (**1**), with vestige of leaf veins shown as ridges on the surface; (**4**) a wedge-shaped leaf; PKUB18803-1; (**5**, **6**) indeterminate plants; (**5**) two axes with longitudinal grooves on surface; PKUB18804; (**6**) axes, with the upper one bearing adventitious roots on one side; PKUB18803-3. Scale bars: (**1, 2, 4, 6**) 10 mm; (**3**) 2 mm; (**5**) 20 mm.

https://doi.org/10.1017/jpa.2021.93 Published online by Cambridge University Press

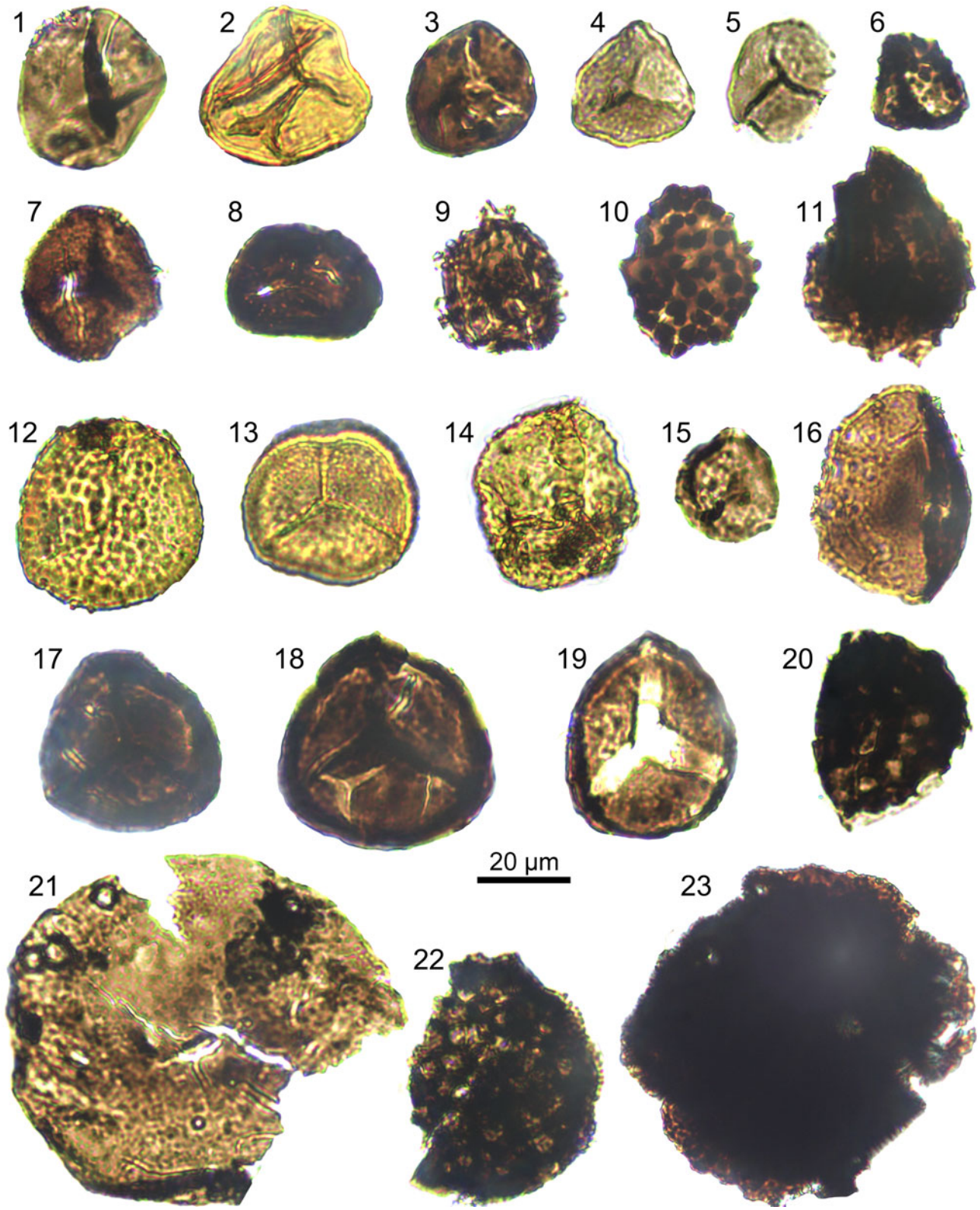


Figure 16. Palynomorphs from bed-10 at section PM90. (**1**) *Gulisporites intropunctatus* Lu, 1981; (**2**) *Gulisporites* sp. 1; (**3**) *Gulisporites hiatus* Lu, 1997; (**4**) *Apiculiretusispora* sp. 1; (**5**) *Aneurospora* sp.; (**6**) *Lophotriletes* sp.; (**7**) *Apiculiretusispora* sp. 2; (**8**) *Densosporites* sp.; (**9**) Acritarch; (**10**) *Dibolisporites* sp.; (**11, 23**) indeterminable spores; (**12**) *Cymbosporites cyathus* Allen, 1965; (**13**) *Cymbosporites conatus* Bharadwaj et al., 1971; (**14**) *Gulisporites* sp. 2; (**15**) *Lycospora* sp.; (**16**) *Retusotriletes* sp.; (**17**, **18**) *Ambitisporites* sp.; (**19**) *Ambitisporites dilutes* (Hoffmeister) Richardson and Lister, 1969; (**20**, **22**) *Reticulatisporites* sp.; (**21**) *Apiculiretusispora* sp. 3.

https://doi.org/10.1017/jpa.2021.93 Published online by Cambridge University Press



Figure 17. Paleogeographic base map modified from B. Huang et al. (2018), showing the localities from which Late Devonian *Archaeopteris* (black dots) and *Melvillipteris* (black squares) are known. Tectonic blocks: IC = Indochina; MOB = Mongolia; NCB = North China; NQ = North Qiangtang; Qm = Qaidam; SCB = South China; SXB = Songliao-Xilinhot. XB, the Xing'an Block, is considered to be a part of the MOB in this reconstruction. JB, the Jiamusi Block, is considered to be a part of the SXB. Localities of *Archaeopteris*: 1, Heihe, Heilongjiang, China (Cai, 1981; locality IX in Table 3); 2, Sonid Zuoqi, Inner Mongolia, China (flag, this study); 3, Southeastern Altay, Russia (Gutak et al., 2011); 4, North Timan, Russia (Orlova et al., 2016); 5, Bear Island, Norway (Nathorst, 1902; Edwards and Berry, 1991); 6, Namur, Belgium (Fairon-Demaret and Leponce, 2001); 7, Kiltorcan Hill, Ireland (Dawson, 1871); 8, Ellesmere Island, Canada (Andrews et al., 1965); 9, New York, USA (Carluccio et al., 1966); 10, Pennsylvania, USA (Beck, 1971); 11, West Virginia, USA (Phillips et al., 1972); 12, Eastern Cordillera, Colombia (Berry et al., 2000); 13, Sierra de Perijá, Venezuela (Berry et al., 2000); 14, Eastern Anti-Atlas, Morocco (Meyer-Berthaud et al., 1999); 15, Eastern Cape, South Africa (Anderson et al., 1995); 16, Nanjing, Jiangsu, China (Wu et al., 1982); 17, Changyang, Hubei, China (Hao and Mei, 1987; Guo and Wang, 2011); 18, Chizhou, Anhui, China (Guo and Wang, 2009); 19, Xinhui, Guangdong, China (Cai et al., 1987); 20, New South Wales, Australia (Young, 2007; Meyer-Berthaud et al., 2016a). Localities of *Melvillipteris*: 2 (this study) and Melville Island, Canadian Arctic Archipelago (Xue and Basinger, 2016).

studies have reported spores from the Angeeryin Ul Formation (Fig. 1.2, Table 3, localities II, III), but the lack of illustrations for these reports prevents a comparison with our results. Spores assigned to 22 genera and 34 species were described from the Heitai Formation of Mishan, Heilongjiang Province, NE China, indicating a Middle Devonian age (Ouyang, 1984), although no taxa at the species level are shared by the Heitai assemblage and that of the PM90 succession.

Another line of evidence for the age of the flora is based upon $^{206}Pb/^{238}U$ ages of detrital zircons from bed-13 (Supplementary Data). The youngest age populations of the measured detrital zircons show a peak value at ca. 365 Ma (Supplementary Data, Fig. 2), within the range of the Famennian Stage (Becker et al., 2020).

Late Devonian plants from blocks of NE China.—Previous records of Late Devonian vascular plants from NE China are sparse, having been described or briefly mentioned from only eight localities, mainly during regional geological surveys during the 1970s and 1980s (Fig. 1.2, Table 3, localities II-IX) (IMBG, 1965, 1973, 1974, 1976; IMBG and NIGS, 1974; HLJBG, 1977, 1981; Cai, 1981; Xue et al., 1982; Wang et al., 2012). Our locality is a new addition to the list. These localities are found on two different crustal blocks: the Xing'an (XB) and Songliao-Xilinhot (SXB) blocks (Fig. 1.2). Among the previously reported plants from XB, two species of *Archaeopteris* from the Xiaohelihe Formation were illustrated and described by Cai (1981) (Fig. 1.2, Table 3, locality IX), while all others have yet to be identified.

The XB is almost, but not precisely, equivalent to the Uliastai active continental margin (Xiao et al., 2003) or the Nuhetdavaa terrane (Badarch et al., 2002), and it may have been a microcontinent since the early Paleozoic (Liu et al., 2017), or even the Neoproterozoic (B. Xu et al., 2015; Zhou et al., 2018). It has been suggested that the XB had become part of the Mongolian Block (MOB) by the Late Devonian, when the MOB occupied a position at 30–60°N (e.g., Fig. 17; based on B. Huang et al., 2018). Thus, the Late Devonian floras of the XB provide data for mid-latitude vegetation of the Northern Hemisphere, which is less well known than lower latitudes.

Four localities on the western segment of the SXB were reported to yield Late Devonian plants from the Seribayan Obo Formation (Fig. 1.2, Table 3, localities V-VIII) (IMBG 1965, 1974; IMBG and NIGS, 1974; Wang et al., 2012). However, only two genera, *Leptophloeum* and *Archaeocalamites*, were recorded, and only the former was illustrated and described.

https://doi.org/10.1017/jpa.2021.93 Published online by Cambridge University Press

Geographically, it seems that during the Late Devonian, the XB was in mid-latitude and the SXB in low-latitude positions (e.g., Fig. 17; B. Huang et al., 2018). A comparison among the Late Devonian floras from the SXB and XB yields the interesting observation that *Leptophloeum* and *Archaeopteris*, two index plants of Late Devonian age, were found in the SXB and XB, respectively, but not in both. Nevertheless, this may well be a result of very limited sampling from both blocks, and such an interpretation would be somewhat premature.

Conclusions

A Late Devonian flora, which is described from a newly discovered locality near Dalai Sumu, northern Sonid Zuoqi, Inner Mongolia, NE China, includes *Melvillipteris sonidia* n. sp., *Archaeopteris* sp., and a possible sphenophyllalean plant. *Melvillipteris sonidia* n. sp. represents the second species of *Melvillipteris*, a genus previously only known from the Upper Devonian (Famennian) of Arctic Canada. *Melvillipteris sonidia* n. sp. is characterized by paired first-order branches that are typically zigzag in appearance; its second-order branches bear three-dimensional sterile ultimate appendages, as well as fertile structures that terminate in fusiform sporangia. An associated palynological assemblage, as well as U-Pb ages of detrital zircon grains from adjacent horizons, are also reported, supporting a Late Devonian age, which in accord with the megafossil plants. Vascular plants have been rarely recorded from Late Devonian deposits of tectonic blocks that constitute present-day NE China. This new flora, from the Xing'an Block, permits comparison with coeval floras from Europe, North America, and South China, and aids our understanding of Late Devonian mid-latitude vegetation of the Northern Hemisphere.

Acknowledgments

The authors thank X.C. Jin for his helpful discussions, and Y.C. Su, Z. Xu, G.D. Qiu, J.X. Du, J.C. Guo, and J.S. Wang for their help with fieldwork and fossil photography. This research was supported by the National Natural Science Foundation of China (Nos. 41722201, 41802003), Geological Survey projects of the China Geological Survey (Nos. DD2016041-15, DD20190008), Strategic Priority Research Program of Chinese Academy of Sciences (No. XDB26000000), and the Natural Science Foundation of Jiangsu Province (No. SBK2018042780). The anonymous reviewers and Associate Editor (J. Nathan) are thanked for their constructive comments that greatly improved the quality of this paper.

Data availability statement

Data available from the Dryad Digital Repository: https://doi.org/10.5061/dryad.d51c5b042

References

Allen, J.R.L., 1964, Studies in fluviatile sedimentation: six cyclothems from the Lower Old Red Sandstone, Anglo Welsh Basin: Sedimentology, v. 3, p. 163–198.

Allen, K.C., 1965, Lower and Middle Devonian spores of north and central Vestspitsbergen: Palaeontology, v. 8, p. 687–748.

Ananiev, A.R., 1960, Studies in the Middle Devonian flora of the Altai-Sayan mountain region: Botanicheskiy Zhurnal, v. 45, p. 649–666. [in Russian with English abstract]

Anderson, H.M., Hiller, N., and Gess, R.W., 1995, *Archaeopteris* (Progymnospermopsida) from the Devonian of southern Africa: Botanical Journal of the Linnean Society, v. 117, p. 305–320.

Andrews, H. N., and Phillips, T. L., 1968, *Rhacophyton* from the Upper Devonian of West Virginia: Botanical Journal of the Linnean Society, v. 61, p. 37–64.

Andrews, H.N., Phillips, T.L., and Radforth, N.W., 1965, Paleobotanical studies in Arctic Canada. I. *Archaeopteris* from Ellesmere Island: Canadian Journal of Botany, v. 43, p. 545–556.

Badarch, G., Dickson Cunningham, W., and Windley, B.F., 2002, A new terrane subdivision for Mongolia: implications for the Phanerozoic crustal growth of Central Asia: Journal of Asian Earth Sciences, v. 21, p. 87–110.

Banks, H.P., 1980, Floral assemblages in the Siluro-Devonian, *in* Dilcher, D.L., and Taylor, T.N., eds., Biostratigraphy of Fossil Plants: Stroudsburg, Dowden, Hutchinson and Ross, p. 1–24.

Bashforth, A.R., and Zodrow, E.L., 2007, Partial reconstruction and palaeoecology of *Sphenophyllum costae* (Middle Pennsylvanian, Nova Scotia, Canada): Bulletin of Geosciences, v. 82, p. 365–382.

Batenburg, L.H., 1982, "Compression species" and "petrifaction species" of *Sphenophyllum* compared: Review of Palaeobotany and Palynology, v. 36, p. 335–359.

Beck, C.B., 1960, The identity of *Archaeopteris* and *Callixylon*: Brittonia, v. 12, p. 351–368.

Beck, C.B., 1971, On the anatomy and morphology of lateral branch systems of *Archaeopteris*: American Journal of Botany, v. 58, p. 758–784.

Beck, C.B., and Wight, D.C., 1988, Progymnosperms, *in* Beck, C.B., ed., Origin and Evolution of Gymnosperms: New York, Columbia University Press, p. 1–84.

Becker, R.T., Marshall, J.E.A., and da Silva, A.C., 2020, The Devonian Period, *in* Gradstein F.M., Ogg, J.G., Schmitz, M.D., Ogg, G.M., eds., Geologic Time Scale 2020 Volume 2: Amsterdam, Elsevier B.V., p. 733–810.

Berry, C.M., and Fairon-Demaret, M., 2001, The Middle Devonian flora revisited, *in* Gensel, P.G., and Edwards, D., eds., Plants Invade the Land: Evolutionary and Environmental Perspectives: New York, Columbia University Press, p. 120–139.

Berry, C.M., and Wang, Y., 2006, *Eocladoxylon* (*Protopteridium*) *minutum* (Halle) Koidzumi from the Middle Devonian of Yunnan, China: an early *Rhacophyton*-like plant? International Journal of Plant Sciences, v. 167, p. 551–566.

Berry, C.M., Morel, E., Mojica, J., and Villarroel, C., 2000, Devonian plants from Colombia, with discussion of their geological and paleogeographical context: Geological Magazine, v. 137, p. 257–268.

Bharadwaj, D.C., Tiwari, R.S., and Venkatachala, B.S., 1971, A Devonian microflora from P'oshi district (Yunnan), China: Palaeobotanist, v. 20, p. 152–169.

Bridge, J.S., 2006, Fluvial facies models: recent developments, *in* Posamentier, H.W., and Walker, R.G., eds., Facies Models Revisited: SEPM Special Publication 84, p. 85–170.

Cai, C.Y., 1981, On the occurrence of *Archaeopteris* in China: Acta Palaeontologica Sinica, v. 1, p. 75–80. [in Chinese with English abstract]

Cai, C.Y., and Wang, Y., 1995, Devonian floras, *in* Li, X.X., Zhou, Z.Y., Cai, C.Y., Sun, G., Ouyang, S., and Deng, L.H., eds., Fossil Floras of China Through the Geological Ages: Guangzhou, Guangdong Science and Technology Press, p. 22–57. [in Chinese]

Cai, C.Y., Wen, Y.G., and Chen, P.Q., 1987, *Archaeopteris* flora from Upper Devonian of Xinhui County, Central Guangdong and its stratigraphical significance: Acta Palaeontologica Sinica, v. 26, p. 55–64. [in Chinese with English abstract]

Carluccio, L.M., Hueber, F.M., and Banks, H.P., 1966, *Archaeopteris macilenta*, anatomy and morphology of its frond: American Journal of Botany, v. 53, p. 719–730.

Cavalier-Smith, T., 1998, A revised six-kingdom system of life: Biological Reviews of the Cambridge Philosophical Society, v. 73, p. 203–266.

Dawson, J.W., 1862, On the flora of the Devonian Period in north-eastern America: Quarterly Journal of the Geological Society of London, v. 18, p. 296–330.

Dawson, J.W., 1871, The Fossil Plants of the Devonian and Upper Silurian Formations of Canada: Montreal, Geological Survey of Canada, 92 p.

Deng, Z.Z., Huang, P., Liu, L., Wang, D.M., and Xue, J.Z., 2016, New observations of *Sphenophyllum pseudotenerrimum* Sze (Sphenopsida) from the Late Devonian of South China: Acta Palaeontologica Sinica, v. 55, p. 45–55. [in Chinese with English Abstract]

Edwards, D., and Berry, C., 1991, Silurian and Devonian, *in* Cleal, C.J., ed., Plant Fossils in Geological Investigation—the Palaeozoic: Chichester, UK, Ellis Horwood, p. 117–153.

Fairon-Demaret, M., 1986, Some uppermost Devonian megafloras: a stratigraphical review: Annales de la Societé Geologique de Belgique, v. 109, p. 43–48.

https://doi.org/10.1017/jpa.2021.93 Published online by Cambridge University Press

Fairon-Demaret, M., and Leponce, I., 2001, Leaf dimorphism in *Archaeopteris roemeriana* (progymnosperm): further early fossil evidence of shoot dorsiventrality: American Journal of Botany, v. 88, p. 729–735.
Fairon-Demaret, M., Leponce, I., and Streel, M., 2001, *Archaeopteris* from the upper Famennian of Belgium: heterospory, nomenclature, and palaeobiogeography: Review of Palaeobotany and Palynology, v. 115, p. 79–97.
Feng, S.N., 1984, Devonian System: plant kingdom, *in* Institute of Geology and Mineral Resources of Yichang, ed., Biostratigraphy of the Yangtze Gorge Area (Vol. III), Late Palaeozoic Era: Beijing, Geological Publishing House, p. 302–303. [in Chinese]
Forbes, E., 1853, On the fossils of the Yellow Sandstone of the South of Ireland: Report of the British Association for the Advancement of Science, v. 22, p. 43.
Galtier, J., and Daviero, V., 1999, Structure and development of *Sphenophyllum oblongifolium* from the upper Carboniferous of France: International Journal of Plant Sciences, v. 160, p. 1021–1033.
Gensel, P.G., 2008, The earliest land plants: Annual Review of Ecology Evolution and Systematics, v. 39, p. 459–477.
Gensel, P.G., and Andrews, H.N., 1984, Plant Life in the Devonian: New York, Praeger Press, 380 p.
Germar, E.F., and Kaulfuss, F., 1831, Über einige merkwürdige Pfanzenabdrücke aus der Steinkohlenformation: Nova Acta Academiae Ceasareae Leopoldino-Carolinae Curiosorum, v. 15, p. 1–230.
Göppert, H.R., 1859, Über die fossile Flora der Silurischen, der Devonischen und unteren Kohlenformation oder des sogenannten Übergangsgebirges: Verhandlungen. der Kaiserlischen Leopoldinisch-Carolinischen Akademie der Naturforscherung, v. 27, p. 425–606.
Gothan, W., and Sze, H.C., 1933, Über die Palaeozoische flora der Provinz Kiangsu: Academia Sinica Memoirs of the National Research Institute of Geology, v. 13, p. 1–40.
Gradziński, R., Baryła, J., Doktor, M., Gmur, D., Gradziński, M., Kędzior, A., Paszkowski, M., Soja, R., Zieliński, T., and Żureke, S., 2003, Vegetation-controlled modern anastomosing system of the upper Narew River (NE Poland) and its sediments: Sedimentary Geology, v. 157, p. 253–276.
Gu, Zhi ("Palaeozoic Plants from China" Writing Group of Nanjing Institute of Geology and Palaeontology, and Institute of Botany, Chinese Academy of Sciences), 1974, Fossil Plants of China, Volume 1. Palaeozoic Plants from China: Beijing, Science Press, 277 p. [in Chinese]
Guo, Y., and Wang, D.M., 2009, *Archaeopteris halliana* from the Late Devonian (Famennian) of Anhui Province, China: Acta Geologica Sinica English Edition, v. 83, p. 479–491.
Guo, Y., and Wang, D.M., 2011, Anatomical reinvestigation of *Archaeopteris macilenta* from the Upper Devonian (Frasnian) of South China: Journal of Systematics and Evolution, v. 49, p. 590–597.
Gutak, J.M., Antonova, V.A., and Ruban, D.A., 2011, Diversity and richness of the Devonian terrestrial plants in the southeastern mountainous Altay (southern Siberia): regional versus global patterns: Palaeogeography, Palaeoclimatology, Palaeoecology, v. 299, p. 240–249.
Hammond, S.E., and Berry, C.M., 2005, A new species of *Tetraxylopteris* (Aneurophytales) from the Devonian of Venezuela: Botanical Journal of the Linnean Society, v. 148, p. 275–303.
Hao, S.G., and Mei, S.L., 1987, Further observations on *Archaeopteris macilenta* Lesquereux from western Hubei: Acta Palaeontologica Sinica, v. 26, p. 555–562. [in Chinese with English abstract]
Hao, S.G., and Xue, J.Z., 2013, The Early Devonian Posongchong Flora of Yunnan—A Contribution to an Understanding of the Evolution and Early Diversification of Vascular Plants: Beijing, Science Press, 366 p.
Hilton, J., 1999, A Late Devonian plant assemblage from the Avon Gorge, west England: taxonomic, phylogenetic and stratigraphic implications. Botanical Journal of the Linnean Society, v. 129, 1–54.
HLJBG (Heilongjiang Bureau of Geology), 1977, Geologic map of the Handaqi: Geological Survey of China, Series M-52-13, scale 1:200,000. [in Chinese]
HLJBG, 1981, Geologic map of the Taerqi: Geological Survey of China, Series M-51-31, scale 1:200,000. [in Chinese]
Hoffmeister, W.S., 1959, Lower Silurian plant spores from Libya: Micropaleontology, v. 5, 331–334.
Huang, B.C., Yan, Y.G., Piper, J.D.A., Zhang, D.H., Yi, Z.Y., Yu, S., and Zhou, T.G., 2018, Paleomagnetic constraints on the paleogeography of the East Asian blocks during late Paleozoic and early Mesozoic times: Earth-Science Reviews, v. 186, p. 8–36.
Huang, P., Liu, L., Qin, M., Liu, L., Deng, Z.Z., Wang, D.M., Basinger, J.F., and Xue, J.Z., 2018, New *Sphenophyllum* plant from the Upper Devonian of Zhejiang Province, China: Historical Biology, v. 30, p. 917–927.
IMBG (Inner Mongolian Bureau of Geology), 1965, Geologic map of the Sonid Zuoqi: Geological Survey of China, Series K-49-6, scale 1:200,000. [in Chinese]
IMBG, 1973, Geologic map of the Dong Ujimqin Qi: Geological Survey of China, Series L-50-21, scale 1:200,000. [in Chinese]
IMBG, 1974, Geologic map of the Honggor Horse Ranch: Geological Survey of China, Series K-50-1, scale 1:200,000. [in Chinese]
IMBG, 1976, Geologic map of the Baolige: Geological Survey of China, Series K-50-22, scale 1:200,000. [in Chinese]
IMBG, 1979, Geologic map of the Dalai: Geological Survey of China, Series L-49-35, scale 1:200,000. [in Chinese]
IMBG, and NIGS (Northeast Institute of Geological Science), 1974, Paleontology Atlas of North China, Inner Mongolia Volume (I): Beijing, Geological Publishing House, 502 p. [in Chinese]
IMBGMR (Inner Mongolian Bureau of Geology and Mineral Resources), 1991, Regional Geology of Inner Mongolian Autonomous Region: Beijing, Geological Publishing House, 726 p. [in Chinese]
IMBGMR, 1996, Multiple Classification and Correlation of the Stratigraphy of China (15), Stratigraphy (Lithostratic) of Inner Mongolian Autonomous Region: Beijing, China University of Geosciences Press, 344 p. [in Chinese]
IMGS (Inner Mongolia of Geological Survey), 2007, Geologic map of the Bayan Ul: Geological Survey of China, Series L49C004004, scale 1:250,000. [in Chinese]
Jongmans, W.J., Gothan, W., and Darrah, W.C., 1937, Beitrage zur Kenntnis der Flora der Pocono-Schichten aus Pennsylvanien und Virginia: Compte Rendus du Deuxième Congrés pour l'avancement des études de Stratigraphie Carbonifère, Heerlen, v. 1935 (1937), p. 423–444.
Kenrick, P., and Crane, P.R., 1997, The Origin and Early Diversification of Land Plants: A Cladistic Study: Washington, DC, Smithsonian Institution Press, 441 p.
Kenrick, P., and Fairon-Demaret., M., 1991, *Archaeopteris roemeriana* (Göppert) sensu Stockmans, 1948 from the upper Famennian of Belgium: anatomy and leaf polymorphism: Bulletin de l'Institut Royal des Sciences Naturelles de Belgique, Sciences de la Terre, v. 61, p. 179–195.
Leclercq, S., 1951, Étude morphologique et anatomique d'une fougère du Dévonien Supérieur, le *Rhacophyton zygopteroides* nov. sp.: Annales de la Société Géologique de Belgique, v. 9, p. 1–62.
Lepekhina, V.G., Petrosyan, N.M., and Radchenko, G.P., 1962, Main Devonian plants of the Altay-Sayan mountain region: Vsesoyuznogo Nauchno-Issledovatel'skogo, Geologicheskogo Instituta (VSEGEI), Trudy, (Novaya Seriya), Leningrad, v. 70, p. 61–190.
Lesquereux, L., 1884, Description of the Coal Flora of the Carboniferous Formation in Pennsylvania and throughout the United States: Geological Survey of Pennsylvania, Report of Progress, v. 3, p. 695–977.
Liu, Y.J., Li, W.M., Feng, Z.Q., Wen, Q.B., Neubauer, F., and Liang, C.Y., 2017, A review of the Paleozoic tectonics in the eastern part of Central Asian Orogenic Belt: Gondwana Research, v. 43, p. 123–148.
Lu, L.C., 1981, Upper Devonian (Frasnian) sporo-pollen assemblages from the Damaidi area of Dukou, Sichuan Province: Bulletin of Nanjing Institute of Geology and Palaeontology, Academia Sinica, v. 3, p. 91–130. [in Chinese with English abstract]
Lu, L.C., 1997, Microflora from Shaodong Member at Jieling section, Hunan, China: Acta Palaeontologica Sinica, v. 36, p. 187–216. [in Chinese with English abstract]
Lu, L.C., 1999, On the miospore assemblages of the Heishantou Formation at Aherbuchomha in Hoboksar, Xinjiang, and with additional reference to the transition stratum from Devonian to Carboniferous, *in* Nanjing Institute of Geology and Palaeontology, ed., Paleozoic Fossils from Northern Xinjiang: Nanjing, Nanjing University Press, p. 1–141. [in Chinese with English abstract]
Makaske, B., 2001, Anastomosing rivers: a review of their classification, origin and sedimentary products: Earth-Science Reviews, v. 53, p. 149–196.
Meyer-Berthaud, B., Scheckler, S.E., and Wendt, J., 1999, *Archaeopteris* is the earliest known modern tree: Nature, v. 398, p. 700–704.
Meyer-Berthaud, B., Decombeix, A.L., Dunstone, R., Gerrienne, P., Momont, N., and Young, G., 2016a, *Tetraxylopteris* Beck emend. Hammond and Berry (2005), the first aneurophytalean genus recorded in Australia: Review of Palaeobotany and Palynology, v. 224, p. 54–65.
Meyer-Berthaud, B., Servais, T., Vecoli, M., and Gerrienne, P., 2016b, The terrestrialization process: a palaeobotanical and palynological perspective: Review of Palaeobotany and Palynology, v. 224, p. 1–3.
Miall, A.D., 1977, A review of the braided-river depositional environment: Earth-Science Reviews, v. 13, p. 1–62.
Nanson, G.C., and Croke, J.C., 1992, A genetic classification of floodplains: Geomorphology, v. 4, p. 459–486.
Nathorst, A.G., 1902, Zur Oberdevonischen Flora der Bären-Insel, Kongl. Svenska Vetenskaps-Akademiens Handlingar, v. 36, p. 1–60.
Nichols, G., 2009, Sedimentology and Stratigraphy: London, Blackwell Science Ltd., 335 p.
Orlova, O.A., Jurina, A.L., and Snigirevsky, S.M., 2016, Late Devonian plant communities of North Russia: Review of Palaeobotany and Palynology, v. 224, p. 94–107.
Ouyang, S., 1984, Microfossils from the Devonian Heitai Formation of Mishan County, Heilongjiang Province: Acta Palaeontologica Sinica, v. 23, p. 69–84. [in Chinese with English abstract]

https://doi.org/10.1017/jpa.2021.93 Published online by Cambridge University Press

Ouyang, S., Lu, L.C., Zhu, H.C., Liu, F., 2017, The Late Paleozoic Spores and Pollen of China: Hefei, China, University of Science and Technology of China Press, 1092 p. [in Chinese with English abstract]
Pettijohn, F.J., 1975, Sedimentary Rocks: Boston, Addison-Wesley Educational Publishers, 736 p.
Phillips, T.L., Andrews, H.N., and Gensel, P.G., 1972, Two heterosporous species of *Archaeopteris* from the Upper Devonian of West Virginia: Palaeontographica, v. 139B, p. 47–71.
Prestianni, C., and Gess, R.W., 2019, *Rinistachya hilleri* gen. et sp. nov. (Sphenophyllales), from the Upper Devonian of South Africa: Organisms Diversity & Evolution, v. 19, p. 1–11.
Richardson, J.B., and Lister, T.R., 1969, Upper Silurian and Lower Devonian spore assemblages from the Welsh Borderland and South Wales: Palaeontology, v. 12, p. 201–252.
Scheckler, S.E., 1986, Geology, floristics and paleoecology of Late Devonian coal swamps from Appalachian Laurentia (U.S.A.): Annales de la Societé Geologique de Belgique, v. 109, p. 209–222.
Schmalhausen, I.F., 1894, Ueber devonische Pflanzen aus dem Donets-Becken: Mémoires du Comité Géologique, v. 8, p. 1–36.
Schweitzer, H.J., 1968, Pflanzenreste aus dem Devon Nord-Westspitzbergens: Palaeontographica, v. 123B, p. 43–75.
Şengör, A.M.C., Natal'in, B.A., and Burtman, V.S., 1993, Evolution of the Altaid tectonic collage and Palaeozoic crustal growth in Eurasia: Nature, v. 364, p. 299–307.
Sinnott, E.W., 1935, Botany, Principles and Problems, Third Edition: New York, McGraw-Hill, 409 p.
Stockmans, F., 1948, Végétaux du Dévonien Supérieur de la Belgique: Mémoires du Musée Royal d'histoire Naturelle de Belgique, v. 110, p. 1–85.
Stur, D., 1875, Die Culmflora des mährisch-schlesischen Dachschiefers: Abhandlungen der Kaiserlich-Königlichen Geologischen Reichsanstalt Wien, v. 8, p. 1–106.
Sze, H.C., 1936, Über die altkarbonische flora der Prov. Kiangsu mit besonderer berücksichtigung des alters des Wutung Quartzites: Bulletin of the Geological Society of China, v. 15, p. 135–164.
Taylor, T.N., Taylor, E.L., and Krings, M., 2009, Paleobotany, the Biology and Evolution of Fossil Plants, Second Edition: San Diego, California, Academic Press, Elsevier, 1230 p.
Tucker, M.E., 2003, Sedimentary Rocks in the Field, Third Edition: Chichester, UK, John Willey and Sons Ltd., 236 p.
Unger, F., 1850, Genera et species plantarum fossilium: Wien, Braunmüller, 627 p.
Wang, D.M., Hao, S.G., and Wang, Q., 2005, *Rotafolia songziensis* gen. et comb. nov., a sphenopsid from the Late Devonian of Hubei, China: Botanical Journal of the Linnean Society, v. 148, p. 21–37.
Wang, D.M., Hao, S.G., Tian, L., and Xue, J.Z., 2006, Further study of the Late Devonian sphenopsid *Hamatophyton verticillatum* from China: International Journal of Plant Sciences, v. 167, p. 885–896.
Wang, D.M, Wan, Z.Z., and Cui, L., 2008, Further study of *Sphenophyllum lungtanense*, with a discussion on the evolution of the Late Devonian Sphenophyllales in South China: Acta Scientiarum Naturalium Universitatis Pekinensis, v. 44, p. 177–194. [in Chinese with English abstract]
Wang, T., Lu, Y.J., Zhang, P.C., and Zhi, X.G., 2012, Revision of the Seribayan Obo Formation in the north of Jarud Qi, Inner Mongolia: Geology and Resources, v. 21, p. 200–204. [in Chinese with English abstract]
Wu, C.Z., Zhao, L.C., and Deng, S.C., 1982, Discovery and significance of *Archaeopteris* in the Wutong Formation near Nanjing Kongshan: Acta Botanica Sinica, v. 24, p. 292–294. [in Chinese]
Xiao, W.J., Windley, B.F., Hao, J., and Zhai, M.G., 2003, Accretion leading to collision and the Permian Solonker suture, Inner Mongolia, China: termination of the central Asian orogenic belt: Tectonics, v. 22, p. 1069–1088.
Xiong, C.H, and Wang, Q., 2008, On the identities of Late Paleozoic *Sphenophyllum* Koenig and *Sphenophyllum* Brongniart (Sphenopsida): Acta Palaeontologica Sinica, v. 47, p. 260–264. [in Chinese with English abstract]
Xu, B., Zhao, P., Wang, Y.Y., Wen, L., Luo, Z.W., Bao, Q.Z., and Zhou, Y.H., 2015, The pre-Devonian tectonic framework of Xing'an-Mongolia orogenic belt (XMOB) in North China: Journal of Asian Earth Sciences, v. 97, p. 183–196.
Xu, H.H., Jiang, Q., Zhang, X.L., Wang, Y., Fu, Q., and Feng, J., 2015, On the Mid Devonian Hujiersite flora from west Junggar, Xinjiang, China, its characteristics, age, palaeoenvironment and palaeophytogeographical significances: Acta Palaeontologica Sinica, v. 54, p. 230–239. [in Chinese with English abstract]
Xue, C.T., Zhao, D., and Zhang, H.R., 1982, Late Devonian and early Carboniferous continental strata in northwestern Xiaohingganling: Journal of Stratigraphy, v. 6, p. 310–311. [in Chinese].
Xue, J.Z., and Basinger, J. F., 2016, *Melvillipteris quadriseriata* gen. et sp. nov., a new plant assigned to Rhacophytales from the Upper Devonian (Famennian) of Arctic Canada: Geological Magazine, v. 53, p. 601–617.
Xue, J.Z., Huang, P., Wang, D.M., Xiong, C.H., Liu, L., and Basinger, J.F., 2018, Silurian–Devonian terrestrial revolution in South China: taxonomy, diversity, and character evolution of vascular plants in a paleogeographically isolated, low-latitude region: Earth-Science Reviews, v. 180, p. 92–125.
Young, G.C., 2007, Devonian formations, vertebrate faunas and age control on the far south coast of New South Wales and adjacent Victoria: Australian Journal of Earth Sciences, v. 54, p. 991–1008.
Zhou, J.B., Wilde, S.A., Zhao, G.C., and Han, J., 2018, Nature and assembly of microcontinental blocks within the Paleo-Asian Ocean: Earth-Science Reviews, v. 186, p. 76–93.
Zimmermann, W., 1930, Die Phylogenie der Pflanzen: Jena, Germany, G. Fischer, 507 p.

Accepted: 8 September 2021

https://doi.org/10.1017/jpa.2021.93 Published online by Cambridge University Press